Multi-Photon Microscopy

Voltage imaging with ANNINE dyes and two-photon microscopy

Christopher J. Roome[1] and Bernd Kuhn[1*]

[1] Okinawa Institute of Science and Technology Graduate University, 1919-1 Tancha, Onna-son, 904-0495 Okinawa, Japan

Corresponding Author: Bernd Kuhn

[*]bkuhn@oist.jp

Running Head: Voltage imaging

Manuscript with

9 Figures

1 Table

Voltage imaging with ANNINE dyes and two-photon microscopy

Christopher J. Roome and Bernd Kuhn

Abstract

Voltage imaging is a tried and tested tool for revealing changes in neuronal membrane voltage at high temporal and spatial resolution *in vitro* and *in vivo*. However, single photon *in vivo* voltage imaging using cameras and synthetic dyes does not allow depth resolution in highly scattering tissue such as the mammalian brain and risks introducing artifacts due to phototoxicity and bleaching. In contrast, voltage imaging with synthetic electrochromic dyes and two-photon excitation near the red spectral edge of absorption circumvents these challenges, allowing depth-resolved measurement of voltage changes at high spatial and temporal resolution in scattering tissue with negligible phototoxicity and bleaching.

Here, we describe how to image voltage using two-photon microscopy and the voltage-sensitive dyes ANNINE-6 and ANNINE-6plus. The key advantages of these dyes are that the voltage response is linear, the temporal resolution is only limited by the imaging speed, and phototoxicity and beaching can be neglected when an excitation wavelength close to the red spectral edge of absorption is chosen. We report how to image membrane voltage of dissociated cells in culture. We provide protocols for imaging average membrane voltage *in vitro* (in brain slices), and in anesthetized and awake animals. Finally, we describe the labeling of single neurons *in vivo* and how to measure supra- and sub-threshold voltage changes in their dendrites in the awake animal. Voltage can be imaged from internally labeled cells for at least two weeks after a single electroporation. Dendritic voltage imaging can be combined with electrical recording, calcium imaging, and/or pharmacology.

Key Words

Voltage-sensitive dye, VSD, voltage imaging, ANNINE, membrane potential, two-photon, *in vitro*, *in vivo*

1. Introduction

Electrical recording has been the key technique for studying neuronal activity, offering accurate voltage and current measurements at high temporal resolution. However, electrical recordings typically suffer from limited spatial resolution. To overcome this problem, in the very early days of functional imaging, L.B. Cohen, B.M. Salzberg, and colleagues screened roughly 1000 synthetic dyes to assess their voltage-sensitivity [1,2]. Based on screening results and/or a mechanistic understanding of fluorescence modulation by membrane voltage, L.M. Loew, A. Grinvald, P. Fromherz, and colleagues developed new and better voltage-sensitive dyes (VSDs) [3-8]. VSDs have since been used with high-speed, low-noise cameras to image modular brain activity *in vitro* and *in vivo* [9,10], voltage changes of single neurons in cell cultures and slice preparations [11-15], and membrane voltage in many other applications [16]. For a recent primer on voltage imaging, see [17].

Genetically encoded voltage indicators have also been developed over the last two decades, each with their own advantages and challenges, but promise to become useful tools in the near future [18,19].

Despite its long history, voltage imaging has remained challenging and has consequently been overshadowed by rapidly developing calcium imaging techniques. This is because voltage signals are typically 10-100 times faster than calcium signals, and thus more difficult to detect. Furthermore, membrane voltage change is spatially restricted to the plasma membrane, whereas calcium concentration changes are detected throughout the intracellular volume. Finally, the signal amplitude of VSDs are much smaller (typically 1/10 or 1/100) than that of calcium indicators.

Phototoxicity and bleaching of VSDs have also been serious drawbacks when voltage imaging from delicate neuronal structures. Therefore, most neuroscientists opt for calcium imaging as a proxy for neuronal activity, despite being limited to supra-threshold events.

Nonetheless, voltage imaging with synthetic voltage dyes offers important advantages over calcium indicators and genetically encoded voltage indicators. Among the wide variety of synthetic voltage indicators, in particular electrochromic VSDs possess several interesting features that render them ideally suited for measuring neuronal membrane potentials. Electrochromic dyes change their color, or, in other words, shift their spectrum due to the electric field over the membrane. This spectral shift is based on a physical effect which does not involve movement of the dye or any type of binding. Therefore, the spectral shift is almost

instantaneous, and so voltage imaging with synthetic electrochromic dyes has a temporal resolution limited only by the imaging speed. In contrast, many genetically encoded voltage indicators have a slower time constant. Additionally, voltage signals measured with synthetic electrochromic dyes are proportional to the membrane voltage. In contrast, calcium signals represent the convolution of the calcium concentration and the binding characteristics of the molecular probe, which introduce delays and nonlinearities. In general, voltage imaging with electrochromic dyes not only reports supra-threshold activity as calcium imaging does, but also sub-threshold activity and hyperpolarization, both of which are essential for understanding the dynamics of dendritic integration and neuronal networks.

Here, we focus on protocols for voltage imaging with two-photon microscopy. This combination allows depth-resolved voltage imaging *in vitro* and *in vivo*. It also reduces phototoxicity and bleaching if the correct excitation wavelength is chosen. We describe cell culture experiments, brain slice experiments, and in vivo experiments with bulk-loaded tissue and single cell labeling.

Additionally, we focus on ANNINE dyes, i.e. ANNINE-6 and ANNINE-6plus, which were developed and designed based on elaborate physical chemistry studies and theoretical models in the laboratory of P. Fromherz at the University of Ulm, Germany, and later at the Max Planck Institute of Biochemistry, Martinsried, Germany [20-23,5,6,24-26]. ANNINE dyes are purely electrochromic, i.e. they exhibit spectral shifts only due to the electric field over the cell membrane but not due to any other effects.

Figure 1 near here

1.1 Mechanism of voltage sensitivity of ANNINE dyes

ANNINE dyes, like other electrochromic VSDs, have a hydrophilic headgroup with electric charges and a hydrophobic tail with no electric charges (Fig. 1a). The headgroup of ANNINE-6 has a positive and a negative charge, while the headgroup of ANNINE-6plus has two positive charges. Due to this design, ANNINE molecules bind to lipid membranes (Fig. 1b).

A second important design feature is that the chromophore, consisting of a ring system and nitrogen atoms, is asymmetric: On one side of the chromophore, the nitrogen is in the ring, on the other side it is outside the ring. Due to this asymmetry, the charges in the chromophore are not symmetrically distributed. Interestingly,

if the chromophore is excited by absorption of a photon, this charge distribution changes. An electron which was in the ground state on one side of the chromophore, moves during the excitation process towards the other side (Fig. 1c). When the dye emits a photon (fluoresces), the electron moves back to the original position.

In the case that the dye molecule is bound to a membrane, the charge shift within the chromophore will interact with the electric field over the membrane. For example, if the negatively charged electron is moved during the absorption process with the electric field over the membrane (the direction of the electric field is defined from plus to minus), then more energy will be needed for the absorption process to occur. This results in a shift of the absorption spectrum to higher energy, i.e. towards shorter wavelength or towards blue. During the emission process, the charge moves back to the original position. But now the charge moves against the external electric field and, therefore, gains energy. Therefore, the emission spectrum is also shifted to shorter wavelengths, and if the electric field over the membrane with the dye molecules changes, the spectral shift will change accordingly. Conversely, if the dye molecules are bound to the opposite side of the membrane, a spectral shift will occur in the opposite direction.

Neurons change their membrane potential if they are electrically active. For example, during an action potential the membrane potential changes from -70 mV at rest to +20 mV. Therefore, if the membrane of a neuron is labeled with a VSD, the neuronal voltage change will shift the spectrum of the voltage sensitive dyes with a linear relation.

The spectral shift must be converted into an intensity change that can be detected with a photomultiplier tube (PMT). Importantly, no intensity change due to a membrane voltage change can be detected if the dye is excited close to the maximum of the excitation spectrum and photons of the full emission spectrum are collected by the PMT. Surprisingly (at first sight), and most importantly, the highest sensitivity (relative fluorescence change per voltage change) of electrochromic dyes, and specifically of ANNINE dyes, is found close to the red spectral edge of absorption [27]. This is true for both one-photon and two-photon excitation (Fig. 1d). As the probability of absorption close to the spectral edge is low, relatively high laser power is necessary for voltage imaging. Fortunately, the required laser power is still low enough not to cause any observable damage.

1.2 Voltage imaging with two-photon excitation

Voltage imaging is always a fight against noise. Optical noise follows the Poisson statistics, so if n photons are detected on average, the expected noise is $\sqrt{n}$. The optical voltage signal (measured in % intensity change) must be larger than the relative noise level ($\sqrt{n}/n$, measured in % intensity fluctuation).

As voltage signals are typically in the range of 0.1 to 10% intensity change, voltage imaging has been in the domain of camera imaging, which enables collection of millions of photons, thereby achieving low relative noise levels. Signals as small as 0.3% relative fluorescence change can be detected in single trials, if more than 1.000.000 photons are detected (relative noise 0.1%) with a signal-to-noise ratio (SNR) of 3. Two- or multi-photon microscopy typically operates in a regime of tens to hundreds of photons. For example, 100 photons result in a relative noise of about 10%. Therefore, so far, only a few studies have been published using two-photon microscopy for voltage imaging [28,29,27,30-32]. A related technique, voltage imaging by second harmonic generation, is similarly challenging [33,17].

One way to increase the number of generated photons is to increase the volume of the excitation point spread function, this however, decreases the spatial resolution. The volume of the point spread function can be increased by underfilling the back focal plane of the objective by introducing a telescope into the laser path, which narrows the beam 2- or 3-fold [34]. An alternative is to use a Bessel module consisting of a spatial light modulator, three lenses and an annular mask to generate an axially elongated Bessel focus [35]. With this technique, the axial excitation can be increase to up to 400 µm.

Another consideration is to convert the linearly polarized excitation light into circularly polarized light by placing a λ/4 plate with the primary axis turned 45° against the direction of the laser polarization into the excitation light path. Thereby, all dye molecules perpendicular to the laser beam axis can be excited and not just those parallel to the original polarization of the laser [36].

Two-photon microscopy is typically slow due to the necessity of scanning the sample. Scanning speed can be increased by line scans and bi-directional scanning. With a galvo scanner, a temporal resolution of up to 2 kHz can be reached by bidirectional line scan. Resonant scanners additionally increase the speed about 15-fold.

Several other fast-scanning two-photon microscopes have been developed and will become important for voltage imaging [37-39]. If no spatial resolution is required, parking the laser beam is an interesting and relatively simple approach to measure voltage at a single location at very high temporal resolution [30].

Another important advantage of two-photon microscopy is that it allows simultaneous excitation of different chromophores due to the wide two-photon absorption spectra. Therefore, for example, voltage and calcium can be imaged simultaneously [36,31]. It is also possible to combine two-photon voltage imaging with other indicators or with membrane bound fluorophores for movement correction.

1.3 Two-photon voltage imaging of cell cultures

In low-density cell cultures, cell membranes are exposed as single sheets. After applying VSD to the bath, voltage imaging can be performed with one-photon excitation (see for example [40]) or two-photon excitation from identified structures (Fig. 1d). If cell cultures get confluent, voltage imaging becomes more difficult as fluorescence signals of different cells might get mixed.

1.4 Two-photon voltage imaging of bulk-loaded tissue

Brain tissue is tightly packed with intermingling cell membranes, as can be seen in any electron microscope image. By applying a VSD non-specifically to the extracellular space, all cell surfaces get labeled. This type of labeling is called bulk-loading. It is impossible to resolve single neurons with one-photon excitation due to the optical resolution limit and scattering. Even depth-resolved imaging is not possible. Two-photon microscopy, however, allows depth-resolved measurement of average membrane potentials and in special cases even signals from single neurons.

Bulk loading can be done by exposing the surface of the brain to a dye solution after removal of the dura [9], by injection of the dye via pipette during an acute experiment [29], by injection of dye via pipette through a PDMS (silicone) membrane covering the craniotomy [41], or, similarly, through a chronic cranial window with an access port [42].

In tissue bulk-loaded with VSD, all cell surfaces of dendrites, axons, somata, and glial cells are labeled. Every membrane-bound dye molecule contributes to the intensity of a measurement, but only those that undergo a membrane voltage change contribute to the signal. Therefore, the signal of voltage imaging is proportional to the ratio of membrane participating in a voltage change to the overall membrane surface in the measured volume and to the amplitude of the voltage change.

Typically, axons show large voltage changes (action potentials), but only for very short times (in mammals, *in vivo*, less than 1 ms) and they contribute a large fraction to the overall neuropil membrane surface. The surface of a single axon is relatively small, and during firing of an action potential, the transient depolarization is typically followed by a slower hyperpolarization. As action potentials are typically not perfectly synchronized, depolarizing and hyperpolarizing signals will cancel out in an average measurement. Therefore, the axonal signal can only be seen under special conditions, as for example, in electrically stimulated parallel fibers of cerebellar slices [43].

Also dendrites contribute a lot to the overall neuropil membrane surface, especially spiny dendrites. Dendritic postsynaptic potentials can synchronize (for example during a sensory input) and are typically slow (several milliseconds) compared to action potentials. Typical voltage changes of postsynaptic potentials in dendrites are 10s of mV. Consequently, their slow, synchronized depolarization makes them the main source of the voltage signal in bulk loaded tissue [44].

Somata barely contribute to the overall membrane potential signal as their surface area is neglectable compared to axons and dendrites. But, surprisingly, it was shown that scanning along the rim of Purkinje neuron somata in cerebellar brain slices yields a signal with a SNR good enough to detect simple spikes in bulk-loaded tissue [31]. However, this might be limited to Purkinje neurons and there are so far no reports of any other cell types where this would be possible.

Glia cells, which contribute significantly to the overall membrane surface, are not expected to participate in fast voltage changes, and, therefore, only dilute the signal.

Statistics on membrane surfaces, i.e., the surface ratio between dendrites, axons, and astrocytes (see for example [45]) help to estimate the expected voltage signal [29]. In most voltage imaging studies, it is assumed that the voltage signal originates from the dendrites only.

Two-photon microscopy allows the measurement of average membrane voltage in response to sensory stimulation, typically after averaging, and average membrane potential oscillations, typically after temporal smoothing [29].

1.5 Two-photon voltage imaging of internally labeled neurons

To overcome the problem of signal mixing in bulk-loaded tissue, it is also possible to load single neurons via a whole-cell recording pipette in slices. This technique was pioneered by S.D. Antic and D.P. Zecevic with electrochromic dyes which have a good water-solubility [11,15]. Cameras can be used for imaging voltage signals from dendrites, somata, and axons. Alternatively, two-photon microscopy can be used for imaging by parking the beam for spot measurements [30] or by scanning short lines [28].

Loading of neurons with VSD is challenging because, on one hand, the dye should bind to the membrane and, on the other hand, it should be soluble during the loading process. As ANNINE-6 is not water-soluble, the less hydrophobic ANNINE-6plus was developed [23]. ANNINE-6plus shares with ANNINE-6 the same chromophore, spectral characteristics, and it is also purely electrochromic [23]. Only the water solubility and membrane affinity are different. ANNINE-6plus saturates at about 1 mM in pure water. However, it precipitates quickly in saline. In general, ANNINE-6plus has a much lower solubility than the JPW dyes [15,11], which are typically used for internal labeling. In our hands, all attempts to fill neurons with ANNINE-6plus in aqueous solutions failed. However, ANNINE-6plus is soluble in ethanol and it saturates at about 6 mM. We were able to fill Purkinje neurons reliably by electroporation with ANNINE-6plus (3 mM) in ethanol. In preliminary experiments, we were also able to label cortical pyramidal neurons with ANNINE-6plus. Purkinje neurons survive this procedure well and the labeling technique subsequently allows reliable supra- and sub-threshold voltage imaging *in vivo* from dendrites for many minutes without bleaching and phototoxic effects [36]. The labeling lasts for at least 2 weeks but, of course, the highest SNR of voltage imaging is found during the first few days after electroporation [36].

In general, there is the concern that VSD bound to intracellular organelle membranes, for example of the endoplasmic reticulum, might dilute the voltage signal by contributing to the fluorescence, but not to the voltage signal [46]. Therefore, the calibration of the relative fluorescence change to voltage should be

considered an approximation. However, for distal Purkinje dendrites, the voltage signals correspond well with dendritic patch-clamp experiments under similar conditions. For example, spikelets of dendritic complex spikes in distal dendrites of Purkinje neurons were estimated to have voltage amplitudes of 34±7 mV [36] with ANNINE-6plus imaging, while patch-clamp experiments under similar conditions resulted in amplitudes of 35±4 mV [47].

2. Materials

Chronic cranial window surgery as described in [48,42,49].

Glass window with access port as described in [42]. For additional advice see Section 3.2.

Two-photon microscope setup

In vivo two-photon microscope setup (e.g., MOM, Sutter Instruments)

Ti:sapphire femtosecond laser (e.g., Coherent or Spectra Physics); for ANNINE-6 and ANNINE-6plus the wavelength range of 950 nm to 1040 nm is important; for voltage imaging we mainly excite at 1020 nm

GaAsP PMTs for high detection quantum yield in combination with low sensitivity above 900 nm (e.g., H10770PA-40, Hamamatsu)

λ/4 plate in the wavelength range of 1020 nm (e.g., WPQW-IR-4M, Sigma-koki)

Telescope (2x or 3x) for narrowing the beam (e.g., BE02R/M, Thorlabs)

Emission filter longpass 540 nm or bandpass 540 nm to 750 nm (e.g., FF01-650/200-25, Semrock); note: if GaAsP PMTs are used no emission filter is needed for excitation wavelengths above 1000 nm

Microscope testing

Fluorescent microbeads (e.g., 19507-5, Fluoresbrite Polychromatic Red Microspheres 0.5 µm, Polyscience)

Agarose Type III-A (A9792, Sigma-Aldrich)

Pipettes for bulk loading, single-cell loading, and electrophysiological recording

Bulk loading: Quartz or borosilicate tubing (e.g., outer diameter 1 mm, inner diameter 0.7 mm; Sutter Instruments)

Single cell loading: Borosilicate tubing (e.g., outer diameter 1 mm, inner diameter 0.58 mm; Sutter Instruments)

Electrophysiological recording:

Quartz electrodes (0.7 mm ID, Sutter Instruments)

Alexa Fluor 594 Hydrazide (A10438, Invitrogen Molecular Probes)

Agarose (A9793, Sigma-Aldrich)

Pipette puller for quartz pipettes (P-2000, Sutter Instruments) or borosilicate tubing (P-2000, P-97, Sutter Instruments)

Beveller (e.g., BV-10, Sutter Instruments)

Injection apparatus for bulk and single-cell loading

Micromanipulator (e.g., MP-285, Sutter Instruments) with pipette holder with port for pressure application (e.g., W.P.I. or HEKA); tower for micromanipulator (e.g., Sutter Instruments)

Bulk loading: Beveled quartz or borosilicate pipettes (10-15 µm opening)

Single-cell loading: Borosilicate pipettes (1 µm tip diameter, 7-10 MΩ impedance measured with saline)

Tubing (typically silicone tubing with 1 mm inner diameter and thick wall) (e.g., from As One, www.as-1.co.jp)

Syringe (fitting to the tubing) preferably with Luer taper (e.g., from As One or W.P.I.)

T-connector (fitting to the tubing) preferably with Luer taper (e.g., from As One or W.P.I.)

3-way (or 4 way) stopcock preferably with Luer taper (e.g., from As One or W.P.I.)

Pressure meter (e.g., PM015R, W.P.I.)

For single-cell loading: Stimulus isolator (ISO-Flex, A.M.P.I.) for electroporation

Preparation of ANNINE-6 and ANNINE-6plus stock solution for bulk and single-cell loading

ANNINE-6 (MW 592.8) or ANNINE-6plus (MW 717.6) (Dr. Hinner & Dr. Hübener Sensitive Farbstoffe GBR, Munich, Germany, http://www.sensitivefarbstoffe.de/; info@sensitivefarbstoffe.de. Alternatively, contact bkuhn@oist.jp)

Desiccator

Vortex

0.22 µm small volume filter (e.g., UFC30GV00, Ultrafree-MC-GV Centrifugal filter 0.22 µm, Millipore)

Small centrifuge

For bulk loading:

DMSO (e.g. Nacalai tesque); DMSO is hygroscopic; to keep DMSO water-free, add molecular sieves 3Å (e.g., 23355-44, Nacalai tesque) to the DMSO bottle

Pluronic F-127 (e.g., AAT Bioquest)

Heater to keep tubes with dye at up to 70°C

For single-cell loading: Ethanol

Solutions

Ringer's solution (135 mM NaCl, 5.4 mM KCl, 1.0 mM $MgCl_2$, 1.8 mM $CaCl_2$,5 mM Hepes (free acid), in H_2O, adjust to pH 7.2 with NaOH)

Saline (150 mM NaCl in H_2O)

3. Methods

3.1 Procedure for voltage imaging with ANNINE-6 in cell cultures

Voltage imaging from dissociated cells in culture is the easiest voltage imaging task and allows imaging of subcellular, cellular, and network voltage changes. The cell membranes are exposed and, therefore, labeling and imaging is relatively easy. In addition, signal amplitudes are high compared to bulk-loaded tissue.

For labeling cell cultures prepare an ANNINE-6 or ANNINE-6plus stock solution by dissolving ANNINE-6 (0.5 mM) or ANNINE-6plus (2.0 mM) in a solution of 20% Pluronic F-127 in DMSO. This stock solution can be kept for a long time (many months) at room temperature if protected from light.

For the labeling solution mix ANNINE-6 or ANNINE-6plus stock solution with saline (0.9% NaCl in water) or Ringer's solution at a ratio of 1:50 or 1:100, respectively. It is important to prepare enough solution to cover the cell culture dish completely with labeling solution to a height of about 2 mm. The labeling solution should be prepared just before labeling the cell culture.

Then, the culture medium of the cell culture dish is removed (but kept in a separate dish) and the labeling solution is added to the cell culture. After 5 minutes the labeling solution is removed, and the cell culture is carefully washed with dye-free saline or Ringer's solution. In most cases washing is not necessary. Enough dye-free saline or Ringer's solution should be added so that the cell culture is well covered (typically a few millimeters). If the labeling is not bright enough the procedure can be repeated, and/or the incubation time can be increased from 5 minutes to 10 minutes.

Now, the cell cultures can be used for voltage imaging with two-photon microscopy or with standard confocal microscopy.

Under the two-photon microscope, only the outline of the cells should be visible. The linearly polarized laser beam will excite parallel-oriented dye molecules but no perpendicularly oriented ones. Spherical cells will have bright poles and a dim equator. This can be overcome by inserting a λ/4 plate into the excitation light path (see Section 3.4)

For cell cultures it is also very convenient to use confocal microscopy for voltage imaging as scattering can be neglected. In most confocal microscopes, laser excitation at 488 nm, 502 nm, and/or 514 nm is available. For these excitation wavelengths, ANNINE-6 and ANNINE-6plus show high sensitivity. In combination with a 540-nm emission longpass filter and line scans along the membrane, voltage imaging can be performed easily.

Figure 2 near here

3.2 Preparation of a cover glass window with access port

Chronic cranial windows are widely used for in vivo imaging [48]. The craniotomy is sealed by a glass cover slip and does not allow access to the brain any more. Here, we describe how to prepare a glass window with access port. The access port allows dye application, drug application, and electrical recording.

The procedure was described before in [42] (Fig. 2a), but in the following paragraphs we give some additional advice for preparing the access port. The windows with access port should be prepared before the surgery and the can be stored for many weeks.

The glass window (typically round with 5 mm diameter) is held with an alligator clip using soft silicone tubing to cover the alligator clip teeth to protect and grip the glass (see Fig. 1 in [42]) . It might be convenient to file down the alligator clip teeth to make the glass more accessible. To reduce the force of clamping, the crocodile clamps can be bent open. The alligator clip can then be mounted on a stand or stereotactic frame, or even held by hand for drilling under a microscope. All drilling is done by hand, on dry glass, using a conical stone drill bit. The free hand is used to blow compressed air on the glass to clear away the glass dust while drilling. To begin making the hole, it is best to drill at higher speed holding the drill at an angle of about 45° to the glass to make an initial hole through the glass with a size of less than 0.5 mm and not necessarily round. It is important to be patient: the glass should always be sanded away rather than chipped. Then the drill is held perpendicular to the glass and the tip of the conical drill bit is inserted into the hole. While using lower drilling speed the glass is grinded to increase the hole size and make a smooth edge. It is best to do this on both sides of the glass to make the hole symmetrical and with perpendicular edges. It is important to avoid creating an angle at the glass edge as this will distort imaging near the hole.

In general, there are several alternative methods for fabricating the hole in any shape and size, for example, sand blasting with a mask or laser-induced etching of fused silica glass. However, sand blasting, in our hands even with the finest grain size, resulted in rough edges. Laser-induced etching is limited to fused silica glass which is expensive but allows cutting of the access port and additionally the shape of the glass cover slip.

Typically, the access port will be off the center. The center of the glass window is reserved for optimal imaging (Fig. 2a).

After drilling the hole, PDMS (typically Sylgard 184) is prepared to fill the hole. To pipette Sylgard, a 1 ml pipette tip is cut with a blade to have an opening of about 4 mm. As it is difficult to pipette a precise volume of Sylgard it is best to measure the weight and add catalyst accordingly at a ratio of 10:1. It is important to mix thoroughly. As the Sylgard/catalyst mixture is not viscous enough to fill the hole it is necessary to heat it first, for example on a glass coverslip over a hot glass bead sterilizer for a few minutes. The Sylgard/catalyst mixture should just be tacky enough to prevent it spreading over the glass window.

Using a 0.5 mm metal drill bit a droplet of tacky Sylgard/catalyst mixture is picked up on the drill bit tip and applied to the glass hole by hand, by inserting the drill bit tip into the hole and carefully allowing the droplet to touch the hole edges. The silicone should only be attached to the inside edges of the hole, lying approximately flat with the glass, and not protrude far above or below the surface of the window. Then the window with the filled hole is heated again, over a glass bead sterilizer for example, to fully set the silicone in the hole. After the silicone is set the window can be cleaned, for example with detergent, and rinsed well with water. Finally, the window is dried with compressed air. The windows with access port should be prepared in advance and can be stored for a long time.

Before mounting the window with access port, it is put into the alligator clip and sterilized above the hot glass bead sterilizer during surgery until it is used. It is important to keep the glass clean, sterile and free of dust.

3.3 Chronic cranial window surgery with access port for *in vivo* imaging

A chronic cranial window with access port is required for *in vivo* imaging of average membrane potential after bulk loading and *in vivo* imaging of voltage from single cells after electroporation.

All animal experiments and genetic manipulations must be approved by local authorities following the respective rules and regulations.

As for any *in vivo* experiment, surgery is crucial for high-quality imaging. Several protocols are available [48,49,42]. Here, we briefly describe our procedure for somatosensory cortex. We anesthetize the mouse with 2-3% isoflurane in air or 100% oxygen in an anesthesia initiation box. Then, we inject dexamethasone (2 mg/kg i.m.) to reduce the immune response and carprofen (7.5 mg/kg i.p.) to reduce inflammation and pain. After shaving the head, we apply hair-removal cream “for sensitive skin” with cotton applicators. The cream dissolves all remaining hair within 2 minutes and should not be applied for too long time to avoid skin irritation. The skin over the future craniotomy is removed. For the craniotomy, a groove is drilled around the target region, leaving a bone patch about 4 mm in diameter intact. It is important to drill until the remaining bone is very thin and flexible, but not so thin as to break through the bone and damage the brain. Bone debris can be removed by careful application of compressed air. To check the thinned bone, slight pressure is applied to the central bone patch and the light reflected off the shiny thinned bone is observed to evaluate if the bone is thin enough. The most critical step of the surgery is to lift the bone. To do this in a controlled way, we glue a tooth pick to the center of the bone patch with superglue or dental acrylic, and then carefully lift the bone without putting pressure on the brain [42]. This technique dramatically increased our success rate of obtaining an intact dura after bone removal (almost 100% success rate for an experienced person).

Then, the window with an access port is mounted, and oriented such that a pipette, which must enter via the access port, can reach the imaging site under the center of the glass at the correct depth. The glass should fit flat on the brain or be pressing it down slightly to reduce movement artifacts during imaging. To do this, it is necessary to remove all bone ridges around the future craniotomy, i.e. the bone patch, before lifting the bone. Also, no bone debris should remain under the glass to avoid bone regrowth. The window is sealed to the bone with superglue. A custom-made headplate (Fig. 2b), light enough to be carried by the animal and strong enough to allow stable head fixation, is fixed to the bone with dental acrylic. As dental acrylic we use MetaBond (also called SuperBond in some countries). The advantage of this dental acrylic is that it bonds very strongly to the skull while other dental acrylics which we tried need a superglue coating of the bone as a mediator. Unfortunately, MetaBond is expensive and only available through dental supply companies (therefore, in some countries, a dental license might be required to buy MetaBond). The wound around the

implant is closed by fixing the skin to the implant with superglue. An analgesic, like buprenorphine, should be injected before the animal awakes. Several days of recovery should be allowed. If the surgery was successful a crisp blood vessel pattern can be seen under the window (Fig. 2c).

Before the VSD injection, it is useful in many cases to map the brain region with imaging of intrinsic signals [50,51,29].

Figure 3 near here

3.4 Two-photon microscope for voltage imaging

In general, any regular two-photon microscope can be used for voltage imaging. However, several specifications and simple modifications can help to increase the SNR (Fig. 3). Care must be taken to follow all laser safety guidelines as infrared high-power femtosecond laser pulses can cause serious damage in the unprotected eye.

As a first modification, a λ/4 plate with the slow or fast axis turned 45° against the polarization direction of the laser can be inserted to convert linearly polarized excitation laser light into circularly polarized light (Fig. 3a). The slow or fast axis of the λ/4 plate is typically marked on the mounting of the plate. Mounting of the λ/4 plate in a rotation mount allows easy adjustment of the angle. The direction of laser polarization can be found in the specifications. After installation, for testing purpose only, a polarizer placed behind the λ/4 plate should not be able to block the laser beam completely. Now all dye molecules with their dipole moment in the plane perpendicular to the light propagation direction, irrespective of how their dipole moments are oriented in the plane, can be excited.

The two-photon point-spread function of excitation is proportional to the numerical aperture (NA) of the objective, laterally by 1/NA and axially by $1/NA^2$ [52]. By increasing the point spread function as described earlier, more dye molecules can be excited; therefore, the SNR can be improved at the expense of spatial resolution. To do this, the back focal plane of the objective can be under-filled by narrowing the excitation laser beam, thereby reducing the effective NA of excitation. Underfilling the back aperture allows using high-NA objectives, which are crucial for efficient fluorescence detection, and at the same time allows excitation of

dye molecules in an increased volume. Typically, the laser beam is decreased to 1/2 or 1/3 with a telescope inserted into the light path between the laser and the microscope.

The point-spread function can be measured by imaging sub-resolution fluorescent microbeads (typically 100 or 200 nm) in a 1.5% agarose gel. To prepare a sample add 1.5% agarose to water and heat while stirring until the agarose dissolves and the foggy emulsion becomes a transparent solution. Then add microbeads (dilute typically 1000-10000 times), stir thoroughly, and add a droplet of the still hot and liquid solution on a glass slide and cover the droplet with a glass cover slip. The agarose will solidify quickly. Now, the test sample can be used with water immersion. It should be possible to find mainly isolated beads. If the bead density is too high, it is necessary to prepare a new sample with higher dilution of the beads. To measure the point spread function a bead is 3D reconstructed with high zoom (typically 5 or higher) and small z-step size (typically 0.5 µm or less).

Some objectives allow adjusting the focal spot with a collar to optimize the point spread function at different depths of imaging in the brain (e.g., XLPLN25XWMP2, 25x N.A. 1.05, Olympus). However, this feature can also be used to artificially widen the point spread function and thereby increase the excitation volume (Fig. 3b).

It is important to use PMTs with high quantum efficiency. GaAsP PMTs typically have a quantum yield 3–5x higher in the visible wavelength range than regular PMTs. As for all two-photon imaging, the PMT sensor size should be large to also collect scattered photons. GaAsP PMTs degrade with exposure to light. Therefore, it is useful to keep a record of laser output, PMT voltage setting, and measured intensity with a specific objective lens of a defined, reproducible sample (e.g. a fluorescein solution with specific molarity). If intensity levels deviate seriously, steps must be taken to find the problem. A spare set of PMTs is typically a good investment and allows for a quick comparison between old and new PMTs.

Emission filters should have as wide a range as possible (for ANNINE-6 or ANNINE-6plus a 540-nm longpass filter), or can be omitted if the PMT is not sensitive to the excitation wavelength, as in the case of GaAsP detectors and excitation wavelengths above 1,000 nm.

Laser stability is crucial for low noise experiments. To test laser stability and noise, a fluorescein solution (about 50 µM can be used, or fluorescent beads visualized in a 1.5% agarose matrix as described above) can be imaged. For example, when imaging a fluorescein solution or a sample with beads for several seconds, a time

course of every pixel in the image can be analyzed. Typically, a wide range of mean intensities will be found as the intensity decreases towards the edges of the image or due to the intensity differences of the imaged structures. If the variance (SD^2) increases linearly with the mean intensity and the extrapolation for intensity = 0 results in variance = 0, then the microscope setup is shot noise limited. The shot noise originates from the photon statistics which follows a Poisson distribution. If a different noise behavior is found it is necessary to search for the noise source (for example, unstable laser, unstable Pockels cell, electronic noise, etc.).

3.5 Injection of VSD into the brain for bulk loading

At first an ANNINE-6 or ANNINE-6plus stock solution should be prepared.

Larger quantities of ANNINE dye can be dissolved in ethanol and then split into convenient aliquots. For example, 1 ml of ethanol is added to a flask containing 0.2 mg ANNINE-6 and 10 aliquots of 100 µl containing 20 ug ANNINE are filled into 500 µl microcentrifuge tubes. After drying the dye in an exicator the tubes can be stored at -20°C protected from light for years.

ANNINE-6 is insoluble in water or saline without additional solvents. ANNINE-6plus dissolves in water to about 1 mM [23]; however, it does not dissolve well in saline. Therefore, a stock solution of ANNINE-6 and ANNINE-6plus is prepared in DMSO at a concentration of 0.5 mM and 2.0 mM, respectively. This corresponds to adding 66 µl of DMSO to a tube with 20 µg ANNINE-6, and 14 µl of DMSO to a tube with 20 µg ANNINE-6plus. Similarly, 20% Pluronic F-127 in DMSO can be used as a solvent. This stock solution can be kept for many months at room temperature protected from light.

Before use, the stock solution (typically a tube with 20 to 200 µl) is heated to 70°C in a water bath or heating block for at least 15 minutes. In general, ANNINE-6 is more difficult to load into tissue at high concentrations, but it persists longer in the tissue than ANNINE-6plus.

Figure 4 near here

To inject the dye into the brain, the PDMS membrane of the access port and the dura mater must be penetrated. This works best with a beveled sharp quartz pipette (Fig. 4a). The angle between the grinding plate

and the pipette axis should be in the range of 25° to 45°; we use 45°. Borosilicate pipettes also work but are less stiff than quartz pipettes. A typical opening is 15 µm for the small diameter of the elliptic opening. To allow a volume measurement, it is useful to draw marks on the pipette trunk to estimate later the volume of injected solution. It can be determined by observing the meniscus and by calculating the volume in the pipette per unit length. For example, when using capillaries with an inner diameter of 0.7 mm, a change of the meniscus by 1 mm corresponds to 385 nL. Typically, 500 to 2000 nL are filled into a pipette and injected into the brain.

Before the experiment, a pipette setup, typically used for patch clamp experiments, should be prepared that allows pressure application and pressure measurement (Fig. 4b). Typically, PVC and/or silicone tubing is used to connect to a 10 mL or 20 mL syringe via a T-connector to a pressure meter. Additionally, a 3-way stopcock should be inserted close to the syringe to control air flow into and out of the tubing and to keep pipette pressure constant by manual control during the injection (Fig. 4c). Before the animal experiment, the apparatus should be tested to determine whether the pipette can reach the access port of the cranial window, whether it fits under the objective that will be used, whether the tubing system holds pressure (test 70 hPa), and whether the markings on the pipette can be observed.

Now an anesthetized mouse can be mounted on the *in vivo* imaging stage. The heated ANNINE-6 or ANNINE-6plus stock solution gets diluted typically 1:50 or 1:20 with saline (0.9% NaCl in H_2O) and backfilled into the pipette. It is best to mix the solution just before filling the pipette, because eventually the dye will precipitate. Then the pipette is mounted on the pipette holder and lowered onto the access port. The approach is observed under a low magnification objective and a region under the access port without major blood vessels is selected. When the pipette tip touches the PDMS (Sylgard) membrane, detected by visual observation, the pipette position is zeroed, and the pipette is slowly lowered along the axis of the pipette through the Sylgard membrane and the dura into the brain. This entry is typically observed by two-photon microscopy imaging of the fluorescent solution in the pipette, but it is recommended to combine it with wide field imaging for better overview and clearer view of the blood vessel pattern. The pipette is moved slowly to allow the brain tissue to relax, typically a few minutes per 100 µm. The target location of the dye delivery is typically between 100 µm and 1000 µm below the pia, which can be judged with the z-focus shift of the two-photon microscope. This can be done under visual control with wide field imaging and/or two-photon microscopy. When reaching the

target location, it is best to wait 5 to 10 minutes so that the tissue can relax and close the gaps between pipette and tissue. Then the pressure in the pipette is slowly increased until the position of the meniscus is changing, as observed by eye or a magnifying glass. The injection should be done slowly and steadily without sharp peaks to keep the tissue as undisturbed as possible. Typically, 1000 nL are injected within 15 minutes (or slower) to label a volume with 400 µm diameter.

For labeling a larger area it is advised to inject at several locations or at several positions along the pipette path through the tissue. For the latter, it is better to do the injections on the path into the tissue, rather than on the way back out, to avoid leakage of the dye to the surface along the injection track. After injection, it is best to wait a few minutes until the dye has bound to the membrane and the pressure in the brain has adjusted to avoid dye solution being squeezed out along the retraction path of the pipette. Then the pipette is slowly retracted and the Sylgard seals the access port again. Now, the animal can recover for a few hours (typically 2 to 12 hours) to allow DMSO to be washed out and the dye to be dispersed evenly.

3.6 Two-photon imaging of average membrane voltage changes *in vivo*

After mounting the mouse again on the *in vivo* stage, either anesthetized or awake, the labeled brain region should be evaluated by two-photon microscopy. This is typically done with a wavelength around 950 nm. The absorption cross-section of ANNINE-6 at 950 nm is higher than in the range of 1020 – 1040 nm (used for functional imaging) and therefore the image is brighter. There should be a clear contrast between the dark cell bodies and the bright neuropil. Bright puncta might be the result of precipitated dye. Also, bright capillaries might be observed. This becomes more obvious a few days after labelling.

Now two-photon voltage imaging can be performed with an excitation wavelength in the range of 1020 - 1040 nm and the appropriate emission filter. Line scans typically show the lowest noise and fluctuation levels and offer a temporal resolution of up to 2 kHz for bi-directional scans with regular galvo scanners. Laser power is typically in the range of 60 mW when imaging close to the surface (cortical layers 1 and 2) and up to 120 mW in deeper layers (cortical layers 3 and 4). Resonant scanners are about 15 times faster and allow box scans (512 x 16 or 512 x 32 pixels per image) at similar temporal resolution (1 kHz or 500 Hz).

Figure 5 near here

One simple way to observe a voltage signal is to apply sensory stimulation. For example, after finding the position of a specific barrel in the somatosensory cortex of the mouse by imaging of intrinsic optical signals (Fig. 5a) and subsequent bulk loading with VSD (Fig. 5b), the principle vibrissa of the barrel can be stimulated. The response can be imaged, and a stimulus-triggered average can be calculated (Fig. 5c). The signal increases with excitation near the red spectral edge of absorption (Fig. 5d). This proves that a voltage change was measured and that the observed intensity change is not a movement artifact.

Sensory responses can be repeatedly applied, which allows stimulus-triggered averaging. Thereby, small signals can be revealed that otherwise would be masked by noise. The software controlling the microscope can supply trigger outputs for synchronizing the stimulus to the imaging. We use ScanImage [53] and MScan (Sutter Instruments).

An alternative is to image sleep spindle activity (Fig. 5e). Sleep spindles are bursts of oscillatory brain activity which occur during stage 2 NREM sleep. Sleep spindles are also observed under anesthesia (e.g., 1.5% isoflurane in oxygen or air, body temperature at 37°C). They are easily recorded electrically with an EEG. To image sleep spindles, the brain region of interest is bulk-loaded with ANNINE-6 or ANNINE-6plus. Then, line scans can be recorded through the cortical tissue depth-resolved due to two-photon excitation (Fig. 5e, line scan position indicated in the images). To increase the SNR, imaging data can be spatio-temporally filtered. For example, Fig. 5e shows a trace where the yellow segment of the line scan was spatially averaged (yellow trace), and then temporally averaged by a box car filter. Additionally, a trace is shown below where the full line scan was spatially averaged and box car filtered. The SNR increases at the expense of spatial and temporal resolution. Voltage imaging of sleep spindles is very useful for testing and comparing imaging setups, surgeries, and dye labeling.

Brain oscillations up to at least 15 Hz can be recorded for hours (recording at 1kHz and subsequent spatio-temporal filtering) without detectable phototoxicity or bleaching. However, for line scans the stability of the preparation is very important as movement artifacts cannot easily be corrected by subsequent alignment during offline analysis. If sequences are going to be averaged, it should be done off-line. This allows sorting out

trials with obvious movement artifacts. The stability of the preparation depends on the brain region, the surgery, and on the position of the mouse on a wheel or ball during the experiment.

Washout of ANNINE-6 is slow, allowing many minutes or even hours of recording. ANNINE-6plus is washed out faster than ANNINE-6. ANNINE-6plus labeling can be considered stable for several hours.

3.7 Analysis of average membrane potential changes during the experiment

Typically, voltage signals are not immediately visible because the relative fluorescence change is smaller and faster than changes observed when, for example, imaging with fluorescent calcium indicators. For a first analysis during the imaging session it is convenient to use a program like ImageJ [54] or FIJI [55] to quickly filter and collapse/average line scans. This gives immediate feedback.

As an example, we show voltage imaging of sleep spindles. After averaging a part of the line scan (indicated by yellow, Fig. 5e), a noisy trace (yellow) is obtained. If the spatio-temporal line scan image is filtered temporally ('Gaussian Blur 3D' of ImageJ and FIJI) and then the line scan segment is averaged, the EEG-correlated membrane depolarization becomes visible (Fig. 5e, black trace overlaying the yellow trace).

3.8 Procedure for *in vitro* voltage imaging after ANNINE-6 labeling *in vivo*

Also for slice experiments, it is recommended to inject ANNINE-6 *in vivo.* The slices can be cut after a few hours. This has the advantage that ANNINE-6 can equilibrate completely, DMSO is washed out, and no precious imaging time is wasted by waiting for adequate labeling to occur after adding dye *in vitro*. Importantly, in our hands, slice labeling (labeling after cutting slices) was not successful because ANNINE-6 and ANNINE-6plus label dead surface cells brightly, while healthy deeper cells remain almost unlabeled.

In this case, surgery can be simplified. After removing hair and mounting the animal in a stereotactic frame, the skin is cut over the target region and pushed aside to expose the bone. Then a 1 mm hole is drilled into the bone. Care should be taken not to drill through the bone. The last layer of bone should be removed with a fine needle tip leaving the dura mater intact. Then, ANNINE-6 can be injected stereotactically (for injection

procedure, see above). For starting parameters, we recommend injecting about 500 nL to 1000 nL of 5% ANNINE-6/DMSO stock solution in saline (prepared after heating of the stock solution for at least 15 min at 70°C). Injection speed should be low (typically 15 minutes for 1000 nL). If necessary, several injections can be made at different depths or in different locations. The injected volume can also be adapted. For sensitive tissue, ANNINE-6/DMSO concentration in saline should be reduced from 5% to 1%.

After injection and retraction of the pipette, the skin is closed again over the craniotomy and either sewed or glued together with superglue. Then the animal can recover. Labeling typically lasts a few days, but it is best to start the *in vitro* experiment (slicing) 2 to 12 hours after injection.

Figure 6 near here

3.9 Two-photon imaging of single-cell membrane voltage changes *in vivo*

Measuring the average membrane potential of bulk loaded tissue with two-photon microscopy is a relatively simple experiment and can be used for mapping depth-resolved postsynaptic potentials *in vivo* or in slice preparations. To understand the neuronal network on a cellular level, one can optically record from single neurons or small networks of neurons *in vivo*, favourably in awake animals. This can be achieved by filling single cells with a VSD, waiting until the dye diffuses and gets incorporated into the membrane, and then image with two-photon microscopy (e.g., while the awake mouse is sitting on a treadmill; Fig. 6a,b). For example, by line-scanning along dendrites, spatio-temporal dendritic voltage maps with sub-millisecond temporal and micrometer spatial resolution can be obtained from cerebellar Purkinje neurons revealing supra- and sub-threshold electrical activity in awake animals [36].

Interestingly, the spectral characteristics of ANNINE-6plus and GCaMP6 allow simultaneous voltage and calcium imaging [36]. Additionally, to record signals at dendritic and somatic locations simultaneously, an extracellular recording electrode can be inserted through the cranial window access port and positioned at the soma to record extracellular spikes, while optical imaging at the dendrites records dendritic activity [36].

In the following we describe how to label and image dendrites of single Purkinje neurons in awake mice with millisecond temporal and several micrometer spatial resolution. It is important to know that Purkinje neurons have about 3 spines per micron at the distal dendrite [56]. This increases the dendritic membrane surface

dramatically such that the spines contribute 80% to the total membrane surface [56]. This huge surface area makes Purkinje neurons a perfect target for voltage imaging. Additionally, the fan-like dendritic tree of Purkinje neurons allows simultaneous line-scanning across several dendritic branches.

At first a chronic cranial window with access port ([42], for further tips see Section 3.2) is mounted over the cerebellum of a mouse (Fig. 6c). A few days after the window surgery, the anesthetized mouse is headfixed on the injection stage. An Adeno-Associated Viral vector (AAV), delivering the gene of GFP, GCaMP, or another green fluorescent chromophore, is injected through the access port into the granule layer of the cerebellum. FITC (50 μM) can also be included in the injection pipette solution to monitor the extent and location of the virus injection under the two-photon microscope. To specifically target Purkinje neurons several promoters or promoter systems are available [57,36]. When the chromophore expression is bright enough, typically after 5 to 10 days, the mouse can be used for targeted labeling of single or multiple Purkinje neurons.

An ANNINE-6plus solution in ethanol is prepared at 3 mM which is half the saturation concentration (Fig. 6d). The solution is shaken using a vortex (10 min) or an ultrasound sonicator (5 min). Then the solution is filtered with a 0.22 μm centrifugal filter.

Mice with a chronic cranial window and access port over the cerebellum are anaesthetized and head mounted. A borosilicate glass patch pipette with 1 μm tip diameter (7-10 MΩ in saline; test pipette resistance first to optimize the pipette pulling; always use fresh pipettes for electroporation) are filled with the ANNINE-6plus/ethanol solution (typically 5 μl; but just enough solution to have electrical contact between the tip of the pipette and the silver wire) and mounted in a pipette holder. The pipette holder has a chlorided silver wire connected to a stimulus isolator. The port of the pipette holder for pressure application is connected to a pressure meter and a syringe. Neutral pressure is applied when entering the brain through the access port to prevent leakage of the dye/ethanol solution into tissue. The ethanol in the pipette prevents clogging of the tip. During the approach of a target cell the pipette tip is visualized with the two-photon microscope. ANNINE-6plus dissolved in ethanol shows bright fluorescence at 1000 nm excitation wavelength and allows positioning of the pipette on a target Purkinje neuron labeled with, for example, GFP or GCaMP6 (Fig. 6e). A slight deformation of the soma should be observed to ensure close contact (Fig. 6e). For electroporation, a stimulus protocol of 50 negative current pulses (-30 μA), 1ms in duration at 100 Hz is delivered (Fig. 6f-h). Neutral

pressure is applied to the patch pipette and the pipette is retracted immediately after the cell is loaded and re-placed for further single-neuron labelling. Typically, several Purkinje neurons can be filled per mouse on the same day. After loading the cells with dye, mice are returned to their cages to allow the dye to spread to distal dendrites and throughout the entire cell. ANNINE-6plus is highly lipophilic, so dye diffusion can take several hours.

After about 20 hours, a brightly labelled Purkinje neuron is selected for the imaging experiment (Fig. 6i,j).

In general, also other cells can be electroporated with this method. For example, we were able to label cortical pyramidal neurons (Fig. 6k). For a first trial, the electroporation parameters should be chosen close to the parameters suggested for Purkinje neurons. Then, pulse amplitude, length, number, and/or frequency can be optimized for best survival of the target cells.

Figure 7 near here

If a labeled cell is selected for imaging, line scans can be performed along the dendritic tree (Fig. 7a). Laser power typically used for imaging dendritic voltage changes in Purkinje neurons at 1020 nm excitation wavelength is in the range of 40 mW to 80 mW. If GCaMP6 is used as a second label, large calcium transients of the dendritic complex spikes can be easily observed. The large calcium transients are associated with the dendritic voltage changes and are therefore reliable indicators of complex spikes. As the absorption cross-section of GCaMP6 at 1020 nm is less than 10% of the peak at 900 nm, ANNINE-6plus and GCaMP6 can be excited simultaneously without bleaching one or the other. In other words, both chromophores are excited close to their red spectral edge of absorption.

By averaging the full line scan spatially, a noise level of less than 5% should be reached. Then, dendritic complex spikes composed of several 1-2 ms spikelets will be clearly visible with fluorescence changes of about 15%.

The labeling lasts for days or even weeks (Fig. 7b,c). However, there is a slow but steady reduction of intensity due to wash out of ANNINE-6plus and therefore a reduction of the SNR. Such long-term experiments suggest that ANNINE-6plus has no serious pharmacological effects on the Purkinje neuron. Also, no bleaching or phototoxicity was observed even after several minutes of line scanning along the Purkinje neuron dendrite.

Figure 8 near here

Using different excitation wavelengths confirms the spectral shift as the mechanism of voltage sensitivity as the relative fluorescence changes increase toward the red spectral edge of absorption (Fig. 8a). As the biological signal varies, multiple measurements are required to average out the biological variability and then to clearly show the wavelength dependent increase in sensitivity (Fig. 8b).

Figure 9 near here

The main advantage of voltage imaging is to obtain spatio-temporal information of voltage changes. With two-photon microscopy, line scans can be recorded with sufficient speed to resolve voltage signals with millisecond precision. For example, by scanning along the dendritic tree of Purkinje neurons, spatio-temporal maps of dendritic voltage (Fig. 9a) and calcium (Fig. 9b) can be imaged. Interestingly, local subthreshold events can be visualized, studied, and quantified in the voltage map (Fig. 9a). Spatio-temporal coherence of a signal (termed hotspot) indicates a voltage change, while a single hot pixel indicates noise.

Additionally, simultaneous extracellular electrical activity can be recorded (Fig. 9c) by using quartz electrodes (0.7 mm ID, Sutter Instruments) beveled at a blunt angle of 40 degrees, with a tip resistance of 7-10 MΩ. To visualize the electrode with the two-photon microscope, 50 µM Alexa Fluor 594 Hydrazide is added to the electrode solution (0.9% NaCl in water). This allows visually guided positioning of the electrode tip, for example, onto the soma of a neuron. To help reduce tip blockage and prevent dye leakage into the tissue electrode tips should be filled with 1-2% agarose gel containing 50 µM Alexa and 0.9% NaCl in water. In this case it is not necessary to apply pressure to the electrode and it can be inserted directly through the silicone access port in the cranial window, with the bath electrode placed above the window under the objective with saline as immersion medium.

To keep some spatial information but to reduce noise, the line-scan can be binned into a few segments. For example, in the dendrites of Purkinje neurons, the number and timing of spikelets in spiny dendrites can be determined with sub-millisecond precision (Fig. 9d).

A very useful tool is *in vivo* pharmacology in combination with simultaneous voltage and calcium imaging. Beveled quartz pipettes (10-15 µm opening) are filled with drug solution and then inserted through the access

port into the brain. The drug is release by pressure application (typically < 20 hPa) through the pressure port of the pipette holder or by iontophoresis.

3.10 Basic off-line analysis of voltage imaging data

Analysis of voltage imaging data can be separated into three consecutive steps: Movement correction, noise reduction by spatial and/or temporal averaging, and calculation of relative fluorescence change.

Movement artifacts should be eliminated as much as possible during the experiment. Movement correction should be not necessary for imaging data from cultures or slices. Unfortunately, in *in vivo* experiments, movement artifacts sometimes cannot be avoided. Some movement artifacts can be corrected or reduced for by shifting lines in line scan data or shifting images in movie data. The shift is determined by cross-correlating each line or image with a reference line or image. The reference line or image is calculated by averaging a segment of the recording with low movement artifacts.

As described in the Introduction, noise can be reduced by increasing the number of photons contributing to a signal. This can be done by adding neighboring pixels and thereby sacrificing spatial resolution (spatial smoothing), or it can be done by adding up data of the same pixel temporally and thereby sacrificing temporal resolution (temporal smoothing). This requires careful consideration of the expected spatial and temporal extent of the measured voltage signal. If not, important features might get filtered out. Typically, regions of interest which are expected to show the same signal are combined to one trace and then temporally averaged. Alternatively, a continuous spatio-temporal filter is applied.

Finally, the relative fluorescence change is calculated. The relative fluorescence change is independent of the brightness of the sample and therefore independent of the number of dye molecules. In general, it reflects the voltage change of the sample. It is calculated by subtracting the baseline fluorescence from the time-dependent fluorescence. The baseline can be a constant,

$$\frac{\Delta F}{F}(t) = \frac{F(t) - F_{baseline}}{F_{baseline}}$$

or the temporally filtered $F(t)$ trace, $F_{baseline}(t)$.

$$\frac{\Delta F}{F}(t) = \frac{F(t) - F_{baseline}(t)}{F_{baseline}(t)}$$

The temporal filtering of $F(t)$ acts as a low-pass filter, and therefore $\frac{\Delta F}{F}(t)$ will only show signals above the cut-off frequency of the temporal filter applied. The filter can be, for example, a sliding box filter.

If other chromophores contribute to the measured intensity or if VSD is bound to membranes that do not participate in a voltage change, then the voltage signal will be "diluted" and therefore be reduced. If autofluorescence or spectral overlap of a second chromophore is known, it can be subtracted as background $F_{background}$.

$$\frac{\Delta F}{F}(t) = \frac{\left(F(t) - F_{background}\right) - \left(F_{baseline}(t) - F_{background}\right)}{F_{baseline}(t) - F_{background}} = \frac{F(t) - F_{baseline}(t)}{F_{baseline}(t) - F_{background}}$$

The relative fluorescence change can then be converted into a voltage change according to Table 1 which results in an estimate of the average membrane voltage change in the spatio-temporal voxel defined by the imaging parameters and the filtering.

If two different chromophores are imaged simultaneously, spectral unmixing might become necessary due to spectral overlap [36]. For an introduction to spectral unmixing see for example[58].

Table 1 near here

3.11 Calibration of relative fluorescence change to voltage

In sparse cell cultures it is possible to calibrate the optical voltage signal to membrane voltage change. The optically measured voltage signal must be compared with an electrical measurement. After labeling the cell culture, patch-clamp electrophysiology in voltage-clamp mode from a cell is used to apply voltage steps via the recording pipette while imaging [27]. Fluorescence changes induced by applied voltage steps can be used to generate a calibration table. An alternative method of applying voltage to cells is to apply external electric fields [27]. It requires a chamber that allows simultaneous imaging and application of electrical fields. This method can be used for high-throughput screening of VSDs to study their characteristics. The conversion table (Table 1) was generated with external electric fields, confirmed with patch clamp technique, and allows to

estimate the voltage change if ANNINE-6 or ANNINE-6plus are excited at 1020 nm or 1040 nm, and a 540-nm emission longpass filter is used for imaging.

In bulk loaded tissue, the voltage signal is “diluted” by the fluorescence of cells not participating in a specific voltage change as cell surfaces are closer to each other than the optical resolution limit (about 40 to 70 nm [59]). Additionally, fine structures like axons and dendrites are tightly intermingled. Therefore, it is only possible to determine the average membrane voltage change in bulk loaded tissue. If an excitation wavelength of 1020 nm or 1040 nm and a 540-nm emission longpass filter is used for imaging, Table 1 allows to determine the average membrane voltage change for a detected relative fluorescence change.

We found that Table 1 can also be used to calibrate voltage signals from dendrites of internally labeled Purkinje neurons. However, it is not clear if this can be generalized to other cell types. The ratio of plasma membrane area to membrane area of organelles will be critical.

4. Trouble Shooting

4.1 Bleaching is observed.

Try to increase the number of dye molecules by using higher dye concentration or a larger volume of dye solution. Reduce laser power. In general, no bleaching should be observed when excited near the red spectral edge of absorption. Check if the PMTs are still sensitive as they might have degraded.

4.2 Imaging intensity is too low.

Try to increase the number of dye molecules by using a higher dye concentration or a larger volume of applied dye solution. Increase laser power. The next possibility is to reduce the excitation wavelength in 10 nm steps starting from 1040 nm. This reduces the sensitivity of the VSD but increases the absorption cross-section. For Ti:sapphire lasers it also increases the output power; therefore, the image becomes brighter. Check if the PMTs are still sensitive as they might have degraded.

4.3 No voltage signals are observed.

If the intensity is too low, then see above. Check noise level of your imaging system. The noise should be shot-noise limited. To test this, record the intensity of a homogeneous fluorescent sample (for example, a dye solution) over time with different laser intensities. Calculate the mean (over time) and corresponding variance of single pixels and groups of pixels for each laser intensity setting and plot variance over mean intensity. For a shot noise limited imaging system, an interpolated line through the data points will cut the coordinate system close to its origin. If the line deviates significantly from the origin, it is necessary to search for the noise source. Calculate a stimulus-triggered average response to reduce noise. Noise decreases with the square root of the number or repetitions. For example, 25 averages reduce the noise to 1/5 of the non-averaged recording. An alternative is to smooth the data spatially, temporally, or spatio-temporally.

5. Outlook

Despite the progress made several problems remain to be solved for two-photon voltage imaging. Labeling single neurons *in vivo* is a challenging technique and requires practice and optimization. Labeling of populations with more than 5 neurons is currently not possible with synthetic dyes. Cell type specific labeling is typically the domain of genetically encoded indicators. However, there are also attempts to combine genetic targeting with synthetic VSDs [60-62]. The basic idea is to express an enzyme in a specific cell type. The synthetic VSD is made water soluble by adding the target group of the enzyme. If the now hydrophilic VSD is exposed to cells expressing the enzyme, the hydrophilic group will be cleaved, the dye becomes hydrophobic, and labels the enzyme-expressing cell. An alternative would be to use the Halo Tag to bind tagged VSD molecules to the membrane [63]. If such processes work under *in vivo* conditions remains to be tested. It would allow use two-photon voltage imaging in a wide range of applications and would make the experiments - hopefully - significantly easier.

Acknowledgement

The authors thank Espen Hartveit, Steven D. Aird, Neil Dalphin, Ray X. Lee, Mohamed M. Eltabbal, Alisher Duspayev, Claudia Cecchetto, and Leonidas Georgiou for valuable feedback on the manuscript and the Okinawa Institute of Science and Technology Graduate University for internal funding.

References

1. Cohen LB, Salzberg BM (1978) Optical measurement of membrane potential. Rev Physiol Bioch P 83:35-88

2. Cohen LB, Salzberg BM, Davila HV, Ross WN, Landowne D, Waggoner AS, Wang CH (1974) Changes in axon fluorescence during activity - Molecular probes of membrane potential. J Membrane Biol 19 (1-2):1-36. doi:Doi 10.1007/Bf01869968

3. Fluhler E, Burnham VG, Loew LM (1985) Spectra, membrane-binding, and potentiometric responses of new charge shift probes. Biochem 24 (21):5749-5755. doi:DOI 10.1021/bi00342a010

4. Grinvald A, Hildesheim R, Farber IC, Anglister L (1982) Improved fluorescent probes for the measurement of rapid changes in membrane potential. Biophys J 39 (3):301-308

5. Hübener G, Lambacher A, Fromherz P (2003) Anellated hemicyanine dyes with large symmetrical solvatochromism of absorption and fluorescence. J Phys Chem B 107 (31):7896-7902. doi:10.1021/jp0345809

6. Kuhn B, Fromherz P (2003) Anellated hemicyanine dyes in a neuron membrane: Molecular Stark effect and optical voltage recording. J Phys Chem B 107 (31):7903-7913. doi:10.1021/jp0345811

7. Loew LM, Bonneville GW, Surow J (1978) Charge shift optical probes of membrane potential - Theory. Biochem 17 (19):4065-4071. doi:DOI 10.1021/bi00612a030

8. Loew LM, Simpson LL (1981) Charge-shift probes of membrane potential - A probable electrochromic mechanism for para-aminostyrylpyridinium probes on a hemispherical lipid bilayer. Biophys J 34 (3):353-365

9. Grinvald A, Frostig RD, Lieke E, Hildesheim R (1988) Optical imaging of neuronal activity. Physiol Rev 68 (4):1285-1366

10. Grinvald A, Hildesheim R (2004) VSDI: A new era in functional imaging of cortical dynamics. Nat Rev Neurosci 5 (11):874-885. doi:10.1038/nrn1536

11. Antic S, Zecevic D (1995) Optical signals from neurons with internally applied voltage-sensitive dyes. J Neurosci 15 (2):1392-1405

12. Palmer LM, Stuart GJ (2006) Site of action potential initiation in layer 5 pyramidal neurons. J Neurosci 26 (6):1854-1863. doi:10.1523/Jneurosci.4812-05.2006

13. Meyer E, Müller CO, Fromherz P (1997) Cable properties of dendrites in hippocampal neurons of the rat mapped by a voltage-sensitive dye. Eur J Neurosci 9 (4):778-785. doi:DOI 10.1111/j.1460-9568.1997.tb01426.x

14. Fromherz P, Müller CA (1994) Cable properties of a straight neurite of a leech neuron probed by a voltage-sensitive dye. Proc Natl Acad Sci U S A 91 (10):4604-4608. doi:DOI 10.1073/pnas.91.10.4604

15. Antic S, Major G, Zecevic D (1999) Fast optical recordings of membrane potential changes from dendrites of pyramidal neurons. J Neurophysiol 82 (3):1615-1621. doi:10.1152/jn.1999.82.3.1615

16. Canepari M, Zecevic D (2010) Membrane potential imaging in the nervous system: Methods and applications. Springer, New York

17. Peterka DS, Takahashi H, Yuste R (2011) Imaging voltage in neurons. Neuron 69 (1):9-21. doi:10.1016/j.neuron.2010.12.010

18. Knöpfel T (2012) Genetically encoded optical indicators for the analysis of neuronal circuits. Nat Rev Neurosci 13 (10):687-700. doi:10.1038/nrn3293

19. Antic SD, Empson RM, Knöpfel T (2016) Voltage imaging to understand connections and functions of neuronal circuits. J Neurophysiol 116 (1):135-152. doi:10.1152/jn.00226.2016

20. Ephardt H, Fromherz P (1993) Fluorescence of amphiphilic hemicyanine dyes without free double-bonds. J Phys Chem 97 (17):4540-4547. doi:DOI 10.1021/j100119a048

21. Fromherz P (1995) Monopole-dipole model for symmetrical solvatochromism of hemicyanine dyes. J Phys Chem 99 (18):7188-7192. doi:DOI 10.1021/j100018a061

22. Fromherz P, Heilemann A (1992) Twisted internal charge-transfer in (aminophenyl)pyridinium. J Phys Chem 96 (17):6864-6866. doi:DOI 10.1021/j100196a004

23. Fromherz P, Hübener G, Kuhn B, Hinner MJ (2008) ANNINE-6plus, a voltage-sensitive dye with good solubility, strong membrane binding and high sensitivity. Eur Biophys J Biophy 37 (4):509-514. doi:10.1007/s00249-007-0210-y

24. Lambacher A, Fromherz P (2001) Orientation of hemicyanine dye in lipid membrane measured by fluorescence interferometry on a silicon chip. J Phys Chem B 105 (2):343-346. doi:DOI 10.1021/jp002843i

25. Röcker C, Heilemann A, Fromherz P (1996) Time-resolved fluorescence of a hemicyanine dye: Dynamics of rotamerism and resolvation. J Phys Chem 100 (30):12172-12177. doi:DOI 10.1021/jp960095k

26. Ephardt H, Fromherz P (1991) Anillnopyridinium - Solvent-dependent fluorescence by intramolecular charge-transfer. J Phys Chem 95 (18):6792-6797. doi:DOI 10.1021/j100171a011

27. Kuhn B, Fromherz P, Denk W (2004) High sensitivity of Stark-shift voltage-sensing dyes by one- or two-photon excitation near the red spectral edge. Biophys J 87 (1):631-639. doi:10.1529/biophysj.104.040477

28. Acker CD, Hoyos E, Loew LM (2016) EPSPs measured in proximal dendritic spines of cortical pyramidal neurons. eNeuro 3 (2). doi:10.1523/ENEURO.0050-15.2016

29. Kuhn B, Denk W, Bruno RM (2008) In vivo two-photon voltage-sensitive dye imaging reveals top-down control of cortical layers 1 and 2 during wakefulness. Proc Natl Acad Sci U S A 105 (21):7588-7593. doi:10.1073/pnas.0802462105

30. Acker CD, Yan P, Loew LM (2011) Single-voxel recording of voltage transients in dendritic spines. Biophys J 101 (2):L11-13. doi:10.1016/j.bpj.2011.06.021

31. Yan P, Acker CD, Zhou WL, Lee P, Bollensdorff C, Negrean A, Lotti J, Sacconi L, Antic SD, Kohl P, Mansvelder HD, Pavone FS, Loew LM (2012) Palette of fluorinated voltage-sensitive hemicyanine dyes. Proc Natl Acad Sci U S A 109 (50):20443-20448. doi:10.1073/pnas.1214850109

32. Fisher JA, Barchi JR, Welle CG, Kim GH, Kosterin P, Obaid AL, Yodh AG, Contreras D, Salzberg BM (2008) Two-photon excitation of potentiometric probes enables optical recording of action

potentials from mammalian nerve terminals in situ. J Neurophysiol 99 (3):1545-1553. doi:10.1152/jn.00929.2007

33. Millard AC, Campagnola PJ, Mohler W, Lewis A, Loew LM (2003) Second harmonic imaging microscopy. Methods Enzymol 361:47-69

34. Helmchen F, Denk W (2005) Deep tissue two-photon microscopy. Nat Methods 2 (12):932-940. doi:10.1038/nmeth818

35. Lu R, Sun W, Liang Y, Kerlin A, Bierfeld J, Seelig JD, Wilson DE, Scholl B, Mohar B, Tanimoto M, Koyama M, Fitzpatrick D, Orger MB, Ji N (2017) Video-rate volumetric functional imaging of the brain at synaptic resolution. Nat Neurosci 20 (4):620-628. doi:10.1038/nn.4516

36. Roome CJ, Kuhn B (2018) Simultaneous dendritic voltage and calcium imaging and somatic recording from Purkinje neurons in awake mice. Nat Commun 9 (1):3388. doi:10.1038/s41467-018-05900-3

37. Nadella KMNS, Ros H, Baragli C, Griffiths VA, Konstantinou G, Koimtzis T, Evans GJ, Kirkby PA, Silver RA (2016) Random-access scanning microscopy for 3D imaging in awake behaving animals. Nature Methods 13 (12):1001-1004. doi:10.1038/Nmeth.4033

38. Reddy GD, Kelleher K, Fink R, Saggau P (2008) Three-dimensional random access multiphoton microscopy for functional imaging of neuronal activity. Nat Neurosci 11 (6):713-720. doi:10.1038/nn.2116

39. Katona G, Szalay G, Maak P, Kaszas A, Veress M, Hillier D, Chiovini B, Vizi ES, Roska B, Rozsa B (2012) Fast two-photon in vivo imaging with three-dimensional random-access scanning in large tissue volumes. Nat Methods 9 (2):201-208. doi:10.1038/nmeth.1851

40. Pages S, Cote D, De Koninck P (2011) Optophysiological approach to resolve neuronal action potentials with high spatial and temporal resolution in cultured neurons. Front Cell Neurosci 5:20. doi:10.3389/fncel.2011.00020

41. Heo C, Park H, Kim YT, Baeg E, Kim YH, Kim SG, Suh M (2016) A soft, transparent, freely accessible cranial window for chronic imaging and electrophysiology. Sci Rep 6:27818. doi:10.1038/srep27818

42. Roome CJ, Kuhn B (2014) Chronic cranial window with access port for repeated cellular manipulations, drug application, and electrophysiology. Front Cell Neurosci 8:379. doi:10.3389/fncel.2014.00379

43. Vranesic I, Iijima T, Ichikawa M, Matsumoto G, Knöpfel T (1994) Signal transmission in the parallel fiber-Purkinje cell system visualized by high-resolution imaging. Proc Natl Acad Sci U S A 91 (26):13014-13017

44. Petersen CC, Grinvald A, Sakmann B (2003) Spatiotemporal dynamics of sensory responses in layer 2/3 of rat barrel cortex measured in vivo by voltage-sensitive dye imaging combined with whole-cell voltage recordings and neuron reconstructions. J Neurosci 23 (4):1298-1309

45. Braitenberg V, Schüz A (1998) Cortex: Statistics and geometry of neuronal connectivity. 2nd edn. Springer, Berlin, New York

46. Djurisic M, Antic S, Chen WR, Zecevic D (2004) Voltage imaging from dendrites of mitral cells: EPSP attenuation and spike trigger zones. J Neurosci 24 (30):6703-6714. doi:10.1523/JNEUROSCI.0307-04.2004

47. Kitamura K, Häusser M (2011) Dendritic calcium signaling triggered by spontaneous and sensory-evoked climbing fiber input to cerebellar Purkinje cells in vivo. J Neurosci 31 (30):10847-10858. doi:10.1523/JNEUROSCI.2525-10.2011

48. Holtmaat A, Bonhoeffer T, Chow DK, Chuckowree J, De Paola V, Hofer SB, Hübener M, Keck T, Knott G, Lee WC, Mostany R, Mrsic-Flogel TD, Nedivi E, Portera-Cailliau C, Svoboda K, Trachtenberg JT, Wilbrecht L (2009) Long-term, high-resolution imaging in the mouse neocortex through a chronic cranial window. Nat Protoc 4 (8):1128-1144. doi:10.1038/nprot.2009.89

49. Mostany R, Portera-Cailliau C (2008) A craniotomy surgery procedure for chronic brain imaging. J Vis Exp (12):e680. doi:10.3791/680

50. Grinvald A, Lieke E, Frostig RD, Gilbert CD, Wiesel TN (1986) Functional architecture of cortex revealed by optical imaging of intrinsic signals. Nature 324 (6095):361-364. doi:10.1038/324361a0

51. Bonhoeffer T, Grinvald A (1996) Optical imaging based on intrinsic signals: The methodology. In: Toga AW, Mazziotta JC (eds) Brain mapping: The methods. 1st edn. Academic Press, San Diego, pp 55-97

52. Theer P, Kuhn B, Keusters D, Denk W (2005) Two-photon microscopy and imaging. In: Meyers RA (ed) Encyclopedia of molecular biology and molecular medicine, vol 15. 2nd edn. VCH, Weinheim Germany ; New York, pp 61-87

53. Pologruto TA, Sabatini BL, Svoboda K (2003) ScanImage: flexible software for operating laser scanning microscopes. Biomed Eng Online 2:13. doi:10.1186/1475-925X-2-13

54. Schneider CA, Rasband WS, Eliceiri KW (2012) NIH Image to ImageJ: 25 years of image analysis. Nat Methods 9 (7):671-675

55. Schindelin J, Arganda-Carreras I, Frise E, Kaynig V, Longair M, Pietzsch T, Preibisch S, Rueden C, Saalfeld S, Schmid B, Tinevez JY, White DJ, Hartenstein V, Eliceiri K, Tomancak P, Cardona A (2012) Fiji: an open-source platform for biological-image analysis. Nat Methods 9 (7):676-682. doi:10.1038/nmeth.2019

56. Vecellio M, Schwaller B, Meyer M, Hunziker W, Celio MR (2000) Alterations in Purkinje cell spines of calbindin D-28 k and parvalbumin knock-out mice. Eur J Neurosci 12 (3):945-954

57. Kuhn B, Ozden I, Lampi Y, Hasan MT, Wang SS (2012) An amplified promoter system for targeted expression of calcium indicator proteins in the cerebellar cortex. Front Neural Circuits 6:49. doi:10.3389/fncir.2012.00049

58. Zimmermann T (2005) Spectral imaging and linear unmixing in light microscopy. Adv Biochem Eng Biot 95:245-265. doi:10.1007/b102216

59. Thorne RG, Nicholson C (2006) In vivo diffusion analysis with quantum dots and dextrans predicts the width of brain extracellular space. Proc Natl Acad Sci U S A 103 (14):5567-5572. doi:10.1073/pnas.0509425103

60. Hinner MJ, Hübener G, Fromherz P (2004) Enzyme-induced staining of biomembranes with voltage-sensitive fluorescent dyes. J Phys Chem B 108 (7):2445-2453. doi:10.1021/jp036811h

61. Hinner MJ, Hübener G, Fromherz P (2006) Genetic targeting of individual cells with a voltage-sensitive dye through enzymatic activation of membrane binding. Chembiochem 7 (3):495-505. doi:10.1002/cbic.200500395

62. Ng DN, Fromherz P (2011) Genetic Targeting of a Voltage-Sensitive Dye by Enzymatic Activation of Phosphonooxymethyl-ammonium Derivative. Acs Chem Biol 6 (5):444-451. doi:10.1021/cb100312d

63. Los GV, Encell LP, McDougall MG, Hartzell DD, Karassina N, Zimprich C, Wood MG, Learish R, Ohana RF, Urh M, Simpson D, Mendez J, Zimmerman K, Otto P, Vidugiris G, Zhu J, Darzins A, Klaubert DH, Bulleit RF, Wood KV (2008) HaloTag: a novel protein labeling technology for cell imaging and protein analysis. Acs Chem Biol 3 (6):373-382. doi:10.1021/cb800025k

Figure Captions

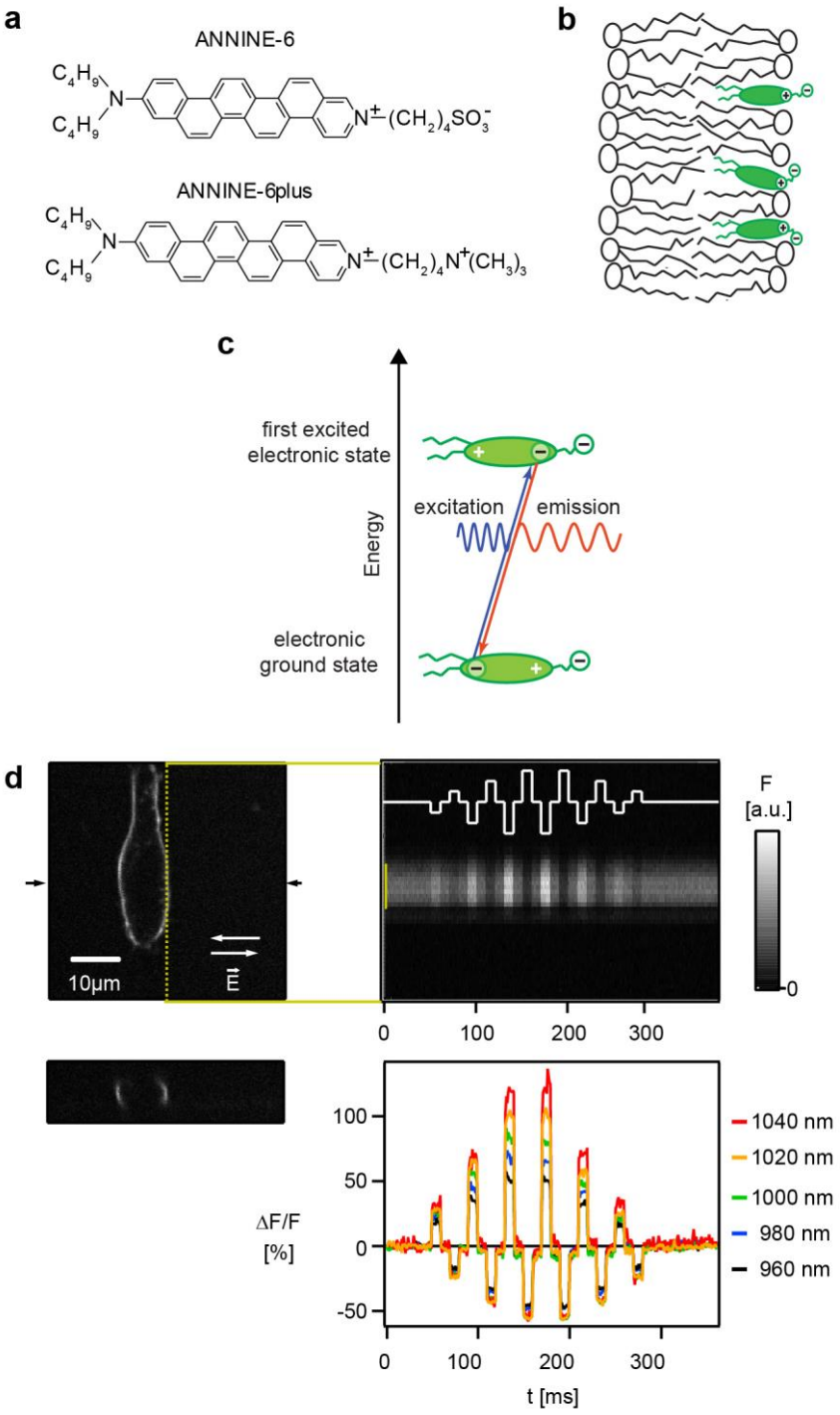

Fig.1 (Kuhn and Roome)

Fig. 1 ANNINE-6 and ANNINE-6plus; basic properties. (**a**) Structure of ANNINE-6 and ANNINE-6plus. Both have a charged and therefore hydrophilic head group (right) and an uncharged hydrophobic tail (left). ANNINE-6plus

is more water soluble than ANNINE-6 due to two positive charges compared to a positive and a negative charge. (**b**) Sketch of a VSD molecules bound to a lipid membrane. The hydrophilic head groups align with the lipid head groups. The hydrophobic tail and chromophore are surrounded by hydrophobic hydrocarbon chains of the lipid molecules. (**c**) Charge shift within a VSD during the absorption and emission process. During the absorption process, the center of charge shifts. This shift occurs due to the asymmetry of the chromophore. (**d**) Relative fluorescence change of ANNINE-6 increases toward the red spectral edge of two-photon absorption. A HEK293 cell labeled with ANNINE-6 is shown in the xy plane and the xz plane at the location indicated by arrows (left). A two-photon line scan was taken along the membrane (yellow dotted line). External electric fields $\vec{E}$ with different amplitudes and direction (white trace, switching directions indicated by white arrows) were applied while scanning along the membrane. The spatio-temporal map shows bright and dark stripes correlating with the applied external electric fields (right). Intensity gray scale is given in arbitrary units [a.u.]. Line scan band (indicated by yellow) was spatially averaged to show relative fluorescence changes corresponding to 6 different (3 positive, 3 negative) membrane voltage changes (bottom). Relative fluorescence changes in response to the same external electric fields increase with increasing excitation wavelength, i.e. closer to the red spectral edge of the absorption spectrum. Modified with permission from Elsevier [27].

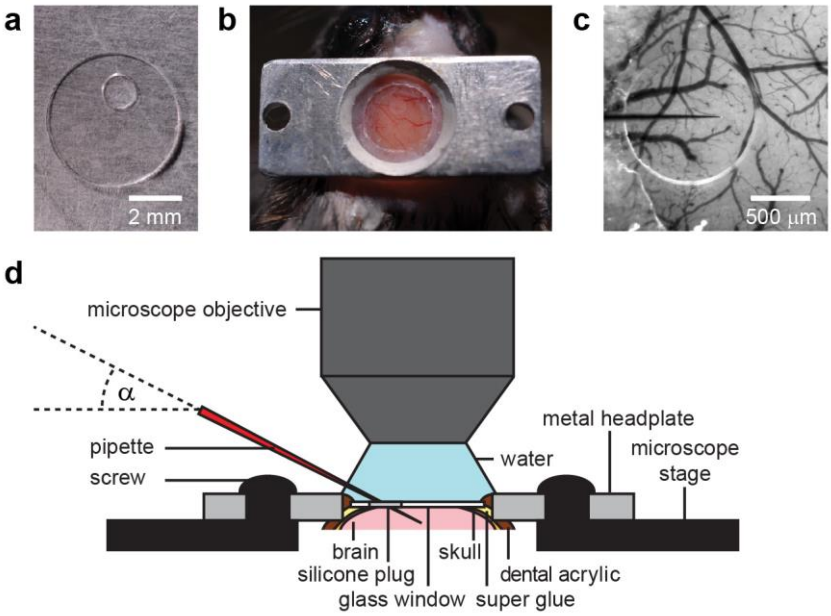

Fig.2 (Kuhn and Roome)

Fig. 2 Chronic cranial window with access port for dye loading, drug application, and electrophysiological recording. (**a**) Glass cover slip with a 1 mm silicone access port. (**b**) Chronic cranial window with an access port can be mounted just as a regular chronic window on top of the dura mater. (**c**) The access port allows repeated brain manipulations for weeks and keeps the imaging site under the glass stable. A dye-filled pipette coming from the left is positioned over a region having only a few blood vessels to avoid bleeding by puncturing vessels. The pipette is then lowered along its axis into the brain. After retraction of the pipette the silicone seals the brain again. (**d**) Schematic of brain manipulation through a chronic cranial window with access port. A typical access angle α is 25°. [42]

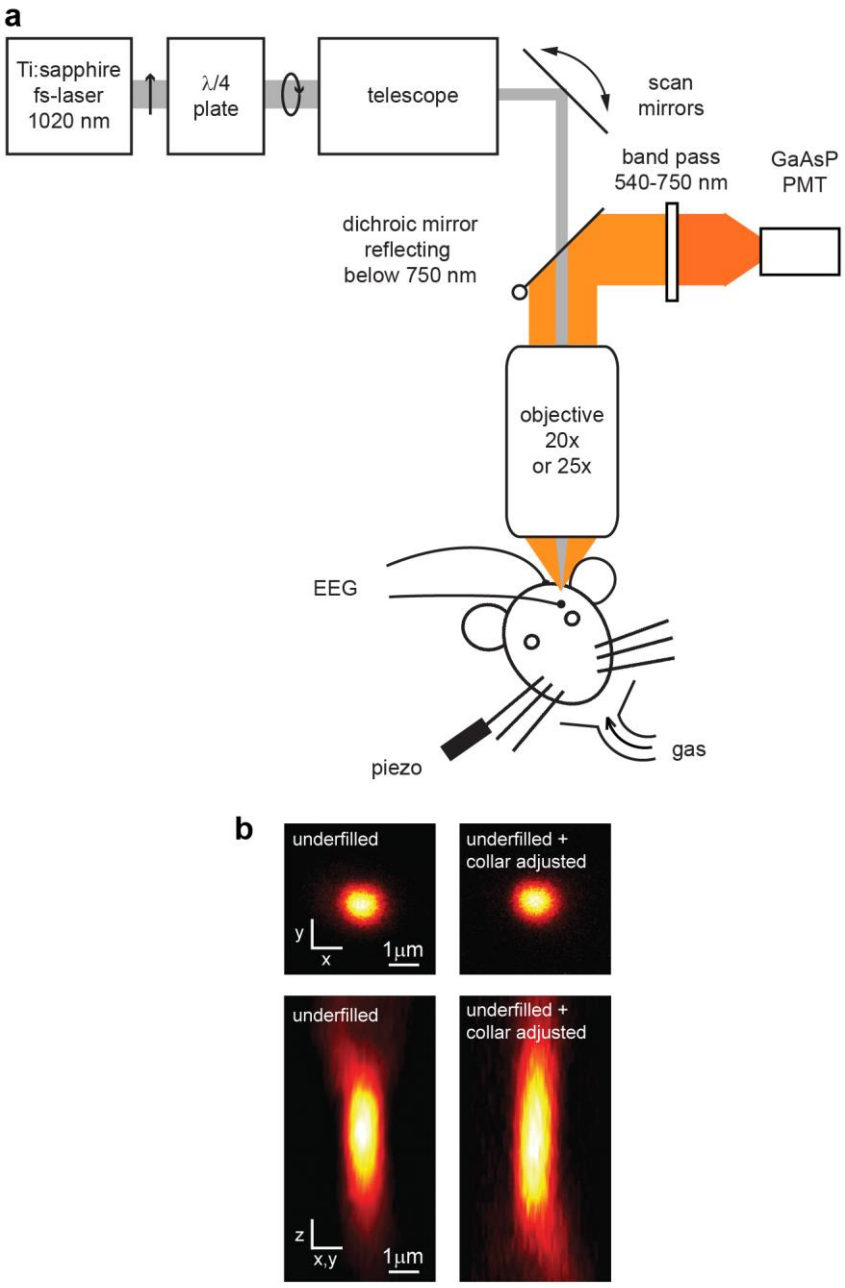

Fig.3 (Kuhn and Roome)

Fig. 3 Schematic drawing of a two-photon microscope for voltage imaging with ANNINE-6 or ANNINE-6plus. (**a**) To optimize voltage imaging, a λ/4 plate and a telescope are inserted into the excitation light path. The λ/4 plate converts the linearly polarized light into circularly polarized light. The telescope decreases the laser beam diameter and thereby underfills the back aperture of the objective. Underfilling the objective's back aperture increases the size of the point spread function of excitation, especially in z-direction, and thereby increases the excitation volume. Larger excitation volume results in more photons and therefore in a reduction of the

relative noise $\sqrt{n}/n$. The objective collects the emitted photons from the sample. Objectives with high numerical aperture are recommended to collect as many photons as possible, again to reduce the relative noise. The dichroic beam splitter and a band pass filter selects the wavelength range of ANNINE-6 or ANNINE-6plus emission with high voltage sensitivity. The GaAsP PMT detects the photons with high quantum yield. Modified with permission from National Academy of Sciences, U.S.A. [29]. (**b**) The excitation volume can be increased by underfilling the back aperture of the objective (left) and, additionally, by turning the collar of the 25x, N.A. 1.05 objective (Olympus) to maximal imaging depth even when imaging close to the surface (right) [36].

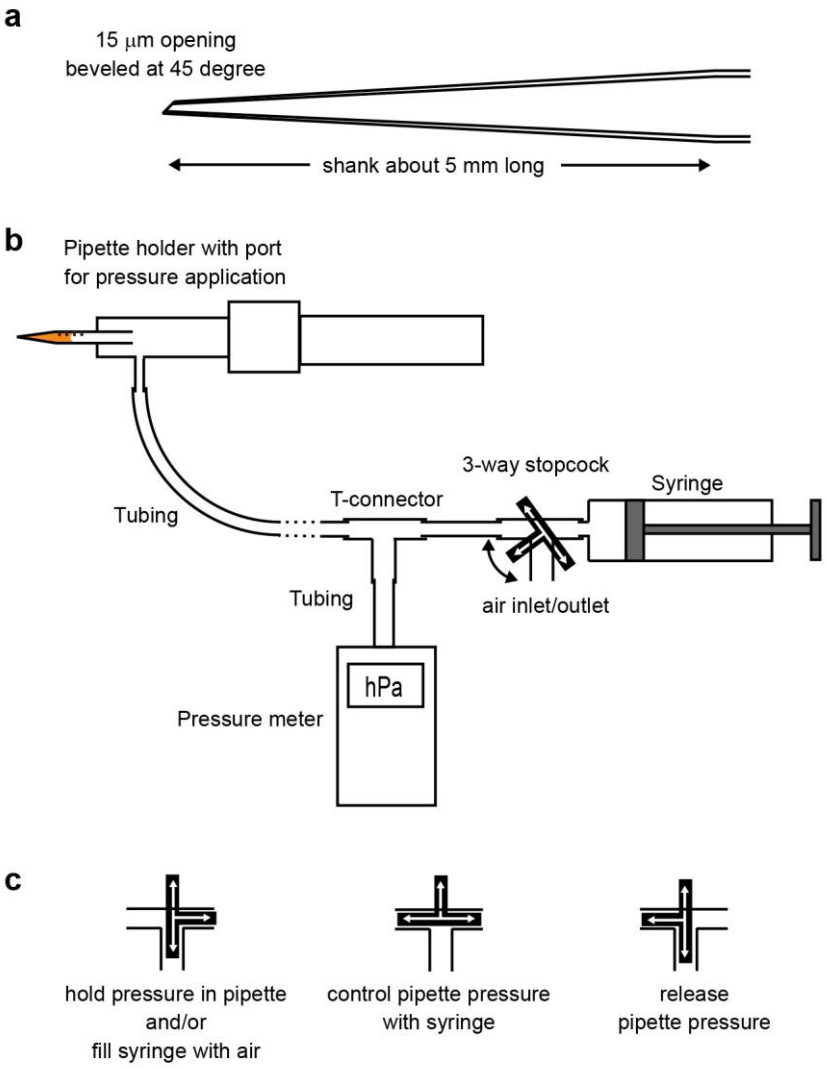

Fig.4 (Kuhn and Roome)

Fig. 4 Equipment for dye pressure injection. (**a**) Sketch of a beveled sharp pipette used for dye injection *in vivo*. (**b**) A 3-way stopcock and a pipette holder with pressure application port allow applying air pressure with a syringe. A manometer is used to measure the pressure during the dye loading. (**c**) Different settings for the 3-way stopcock in (**b**). The arrows on the 3-way stopcocks indicate the air flow directions during different procedures.

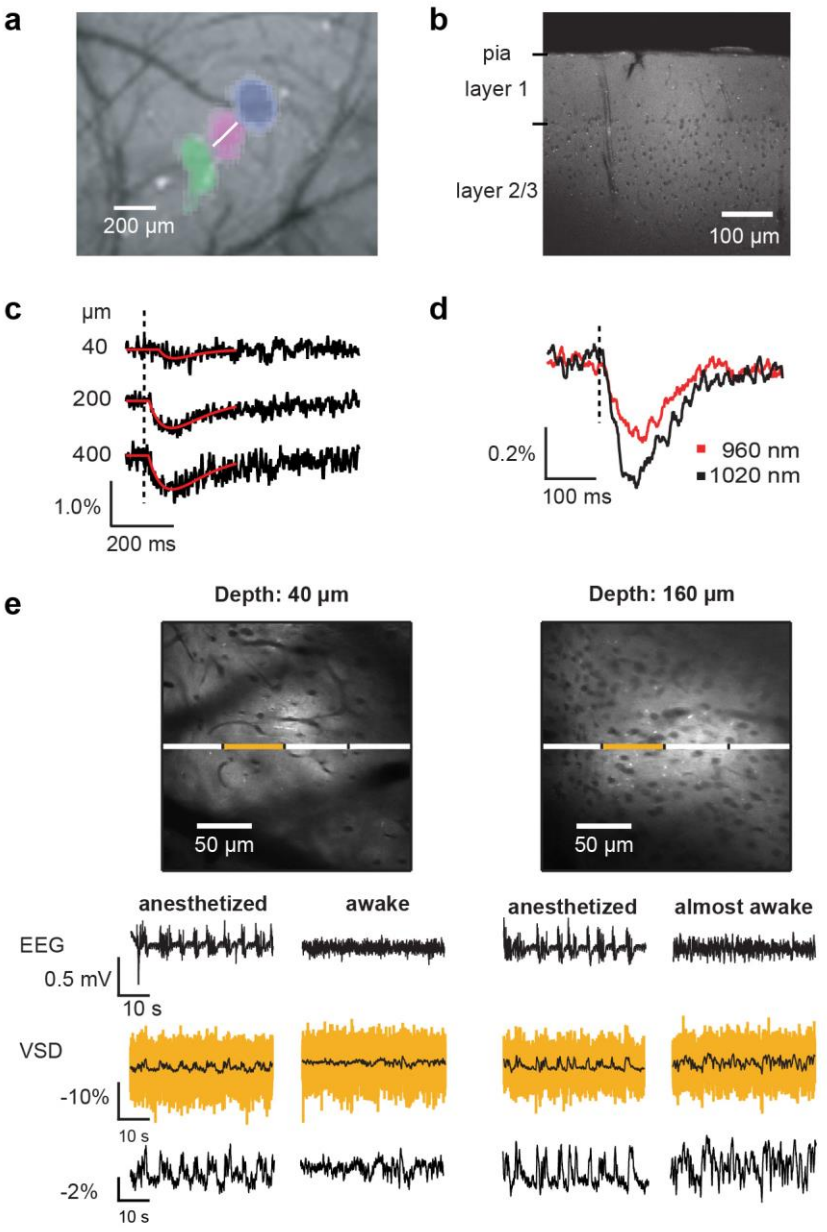

Fig.5 (Kuhn and Roome)

Fig. 5 Voltage imaging of average membrane potential of neuronal tissue *in vivo*. (**a**) Imaging of intrinsic signals reveals the location of primary responses in barrel cortex. In this montage, three vibrissa responses (green, magenta, blue) in relation to the blood vessel pattern are shown. Following the imaging of intrinsic signals, the brain region of interest was bulk loaded with VSD. (**b**) Two-photon image of a barrel cortex brain slice prepared after *in vivo* bulk-loading with ANNINE-6 shows homogeneous labeling. Somata (here of layer 2/3) and blood vessels remain dark. (**c**) Two-photon line scans performed at the location indicated in (**a**) (white line) at different depths below the brain surface were spatially averaged. Vibrissa stimulation causes an average

membrane depolarization, which results in decrease of fluorescence if the dye is bound to the outer leaflet of the membrane and the dye is excited at the red spectral absorption edge. (**d**) Under the same experimental conditions, the excitation wavelength was changed. As expected from a purely electrochromic dye, excitation closer to the spectral edge results in a larger relative fluorescence change. Such an experiment confirms the mechanism of voltage sensing. (**e**) *In vivo* two-photon images of cerebral cortex layer 1 and layer 2/3. Blood vessels and somata appear as dark shadows, as the dye is bound to the outer leaflet of the cell membranes. Line scans allow measurement of local average membrane depolarization in anesthetized and awake animals, which correlates with the local electro-encephalogram (EEG). The yellow trace is the averaged trace of the line scan segment indicated above. The black, overlaid trace is the corresponding filtered trace (boxcar smoothing, 200 ms). The segmentation allows analyzing cross-correlations among neighboring brain segments. For example, cross-correlations among segments are higher in anesthetized than in awake animals [29]. The trace at the bottom shows the relative fluorescence change of the full line scan after filtering with 200 ms boxcar smoothing. EEG signals are biphasic, representing sources and sinks while the VSD signal shows average membrane depolarization (negative fluorescence change). As the neuronal activity de-correlates during the transition from anesthetized to awake state, the average voltage signal becomes noisy (160 µm below the dura mater, right VSD traces) and then flat (40 µm, right VSD traces) in the fully awake animal. Average membrane voltage measurements can be recorded for hours without photo bleaching. Modified with permission from National Academy of Sciences, U.S.A. [29].

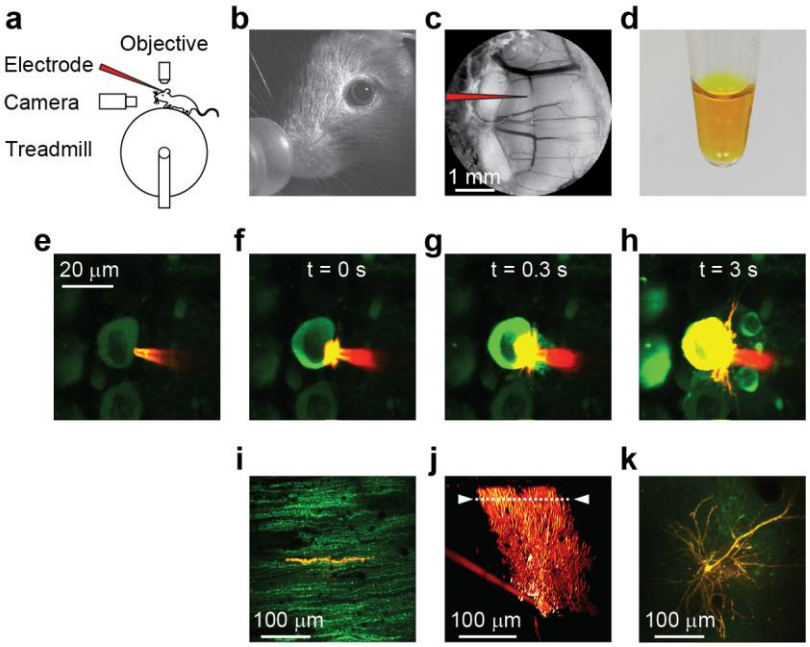

Fig.6 (Kuhn and Roome)

Fig. 6 Dual labelling of an individual Purkinje neuron for combined voltage and calcium two-photon imaging in awake mice. (**a**) Sketch of the setup with a mouse mounted on a treadmill under a two-photon microscope. An electrode is used to fill single Purkinje neurons by electroporation and to electrically record from their soma. (**b**) A behavioral camera allows detailed observation of the pupil, the vibrissa, and the face of the mouse. (**c**) A chronic cranial window with access port on the vermis of the cerebellum allows entering the brain with a pipette (schematically indicated). (**d**) ANNINE-6plus dissolved in pure ethanol at 3 mM concentration. (**e**) A patch pipette filled with ANNINE-6plus in ethanol is used to label single GCaMP6f expressing Purkinje neurons by electroporation in the anesthetized mouse. (**f**-**h**) shows a GCaMP6f labelled Purkinje neuron filled at the soma with ANNINE-6plus by electroporation, at t = 0, 0.3, and 3 seconds, respectively. 24 hours after labeling a Purkinje neuron with ANNINE-6plus, the dye spread out evenly as can be seen (**i**) in the cross-section of the Purkinje neuron dendrite as an overlay of the green channel (GCaMP6f) and the red channel (ANNINE-6plus). (**j**) Reconstruction of the Purkinje neuron in the red channel (ANNINE-6plus). (k) It is also possible to label cortical pyramidal neurons with ANNINE-6plus by electroporation. The image shows a z-projection of a layer 3 pyramidal neuron. Modified from [36].

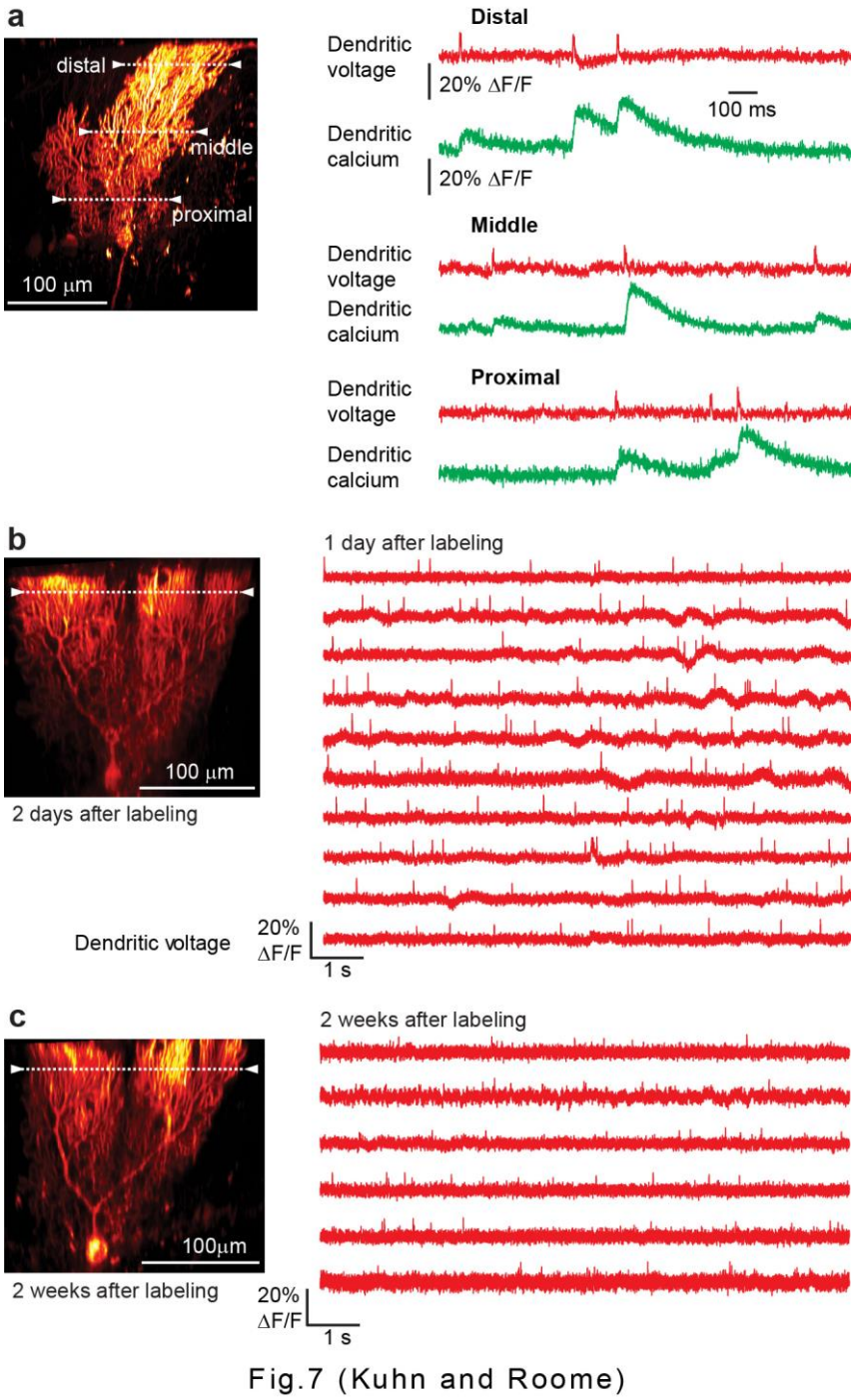

Fig.7 (Kuhn and Roome)

Fig. 7 Simultaneous voltage and calcium imaging of dendritic activity in a Purkinje neuron and long-term imaging. (**a**) Reconstruction of a Purkinje neuron one day after labeling with ANNINE-6plus. The GCaMP labeled Purkinje neuron was filled with the dye by targeted electroporation. Averaged line scans along the distal and proximal dendrite at the position indicated (left) show rapid voltage depolarization events in the red channel (red traces) and long-lasting calcium transients in the green channel (green traces). The signals correspond to dendritic complex spikes. As ANNINE-6plus is applied internally, depolarization results in a

positive fluorescence change when excited at the red spectral edge of absorption. Note, the signal direction is inverted compared to extracellular labeling (e.g. see Fig. 5c). (**b**) Reconstruction of a Purkinje neuron two days and (**c**) two weeks after electroporation with ANNINE-6plus. Spatially averaged, uncorrected recordings of dendritic voltage one day and 2 weeks after labeling (right) at location indicated (left) show reliable dendritic complex spike detection but no bleaching or phototoxicity. The SNR in the later recording decreased in comparison to the earlier one. All line scans were recorded at 2 kHz. [36]

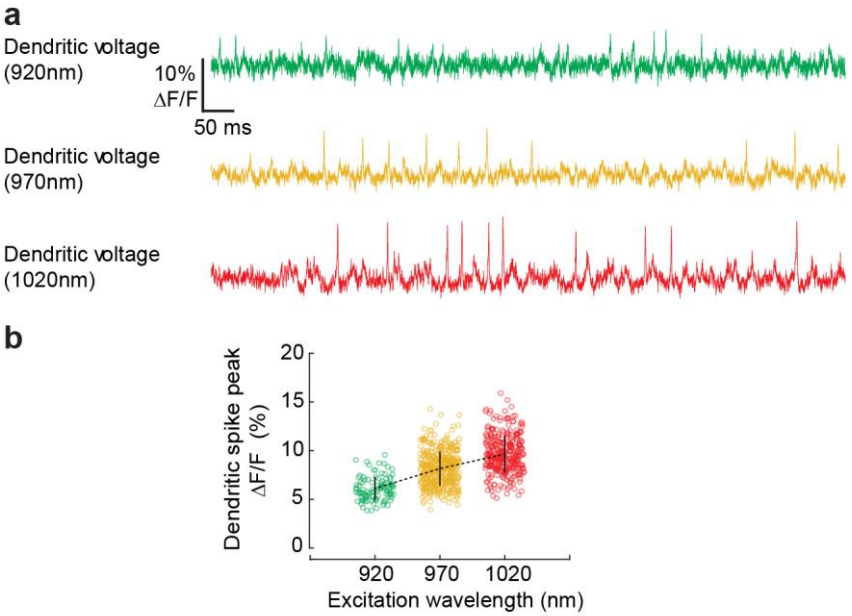

Fig.8 (Kuhn and Roome)

Fig. 8 Relative fluorescence change is excitation wavelength dependent, as shown before in HEK293 cell cultures (Fig. 1d). (**a**) Averaged line scan recordings from distal spiny dendrites of a Purkinje neuron in an awake mouse with excitation wavelength of 920 nm, 970 nm, and 1020 nm. (**b**) The peak amplitudes of dendritic complex spikes fluctuate due to biological variability for each excitation wavelength. The mean signal increases with excitation closer to the red spectral edge of absorption confirming the mechanism of voltage-sensitivity, i.e. the spectral shift. [36]

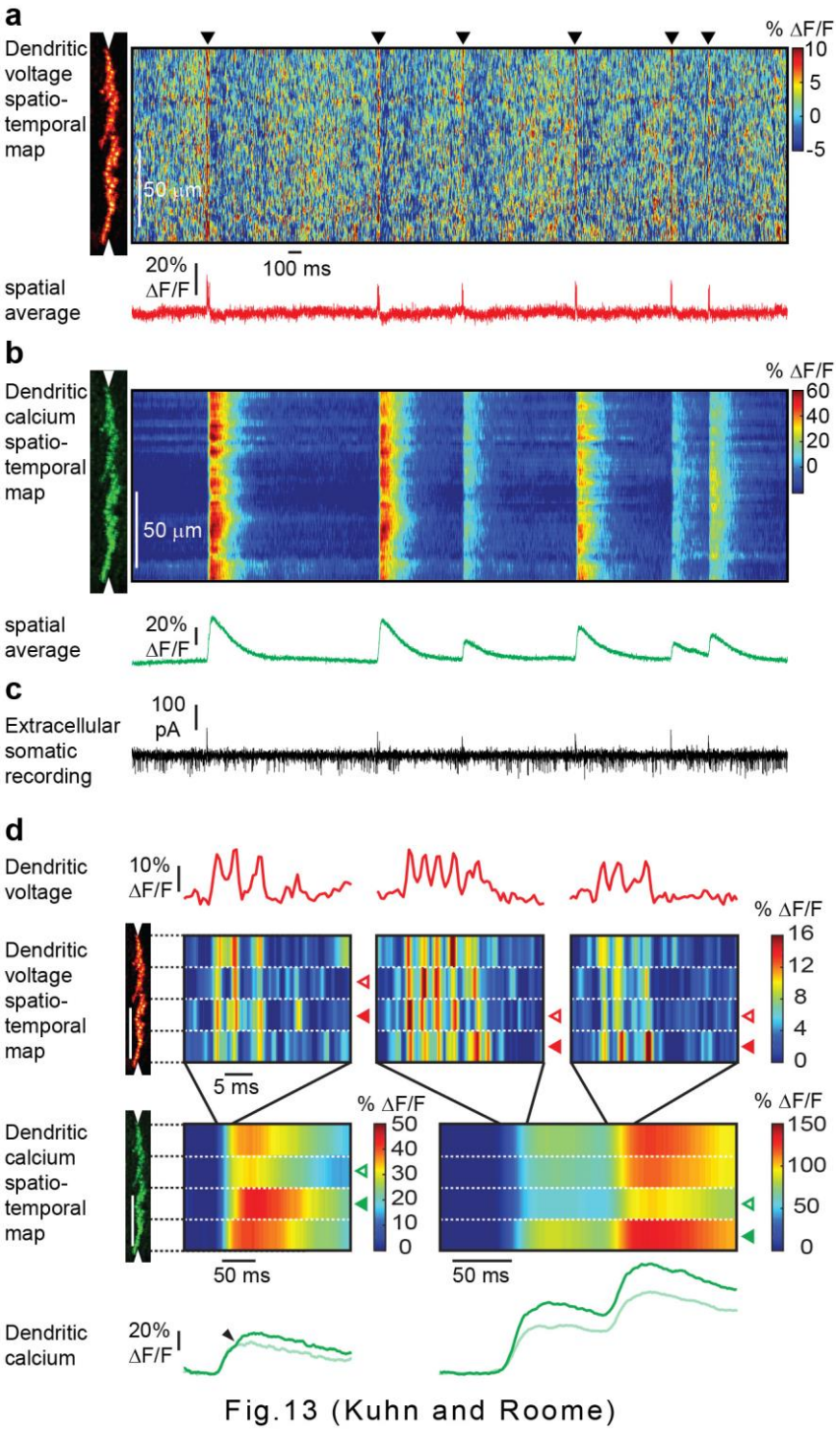

Fig.13 (Kuhn and Roome)

Fig. 9 Simultaneous voltage and calcium imaging of Purkinje neuron dendrites and electric recording from the soma in the awake mouse. (**a**) A line scan at 2 kHz was taken along the Purkinje neuron dendrite (left) to measure a voltage spatio-temporal map in an awake mouse. Note red vertical lines (black triangles) indicating activation of the full dendritic tree during a complex spike, and background pattern with red hotspots indicating localized subthreshold electrical activity. The spatially averaged dendritic voltage trace shows

dendritic complex spikes at high SNR. (**b**) The corresponding dendritic calcium spatio-temporal map shows large transients for every dendritic complex spike. Note the spatial variability of the peak amplitude of calcium transients within single dendritic complex spikes and the amplitude variability between different dendritic complex spikes. (**c**) The access port allowed simultaneous extracellular electrical recordings from the soma while imaging voltage and calcium transients from the dendrites. Simple spikes (somatic Na^+ spikes) result in a current sink at the soma, while complex spikes (dendritic Ca^{2+} spikes) result in a dominant current source signal at the soma. (**d**) Different parts of the dendritic tree show a different number of spikelets during the same complex spike event. The number of spikelets correlate with the amplitude of the calcium transients in each part of the dendritic tree. Open arrowheads indicate spatially localized low activity, filled arrowheads high activity. Spatially localized dendritic spikelets during complex spikes correlate with a local boost in the dendritic calcium transient (small arrowheads). Note that the depolarization is caused by the influx of Ca^{2+}. Therefore, the voltage and calcium signal should have the same onset. The observed delay in onset of the calcium signal is the result of the dynamics of the calcium indicator GCaMP6f. [36]

Table 1: Conversion of relative fluorescence change (%) to voltage for ANNINE-6 or ANNINE-6plus in the outer membrane leaflet (bath application of the dye) at an excitation wavelengths of 1020 nm or 1040 nm using a 540-nm emission longpass filter. If the dye is internally applied, the sign of the relative fluorescence change must be inverted to read the correct voltage.

Table 1

Relative Fluorescence Change [%]	Excitation at 1020 nm: Membrane potential change [mV]	Excitation at 1040 nm Membrane potential change [mV]
50	-74	-68
40	-62	-57
30	-48	-44
20	-34	-31
10	-18	-16
0	0	0
-10	19	18
-20	41	38
-30	65	60
-40	94	85
-50	127	117